arXiv:0909.3025v1 [astro-ph.GA] 16 Sep 2009

Does Stellar Feedback Create HI Holes? An HST/VLA Study of Holmberg II

Daniel R. Weisz, Evan D. Skillman

Astronomy Department, University of Minnesota, Minneapolis, MN 55455

`dweisz@astro.umn.edu, skillman@astro.umn.edu`

John M. Cannon

Department of Physics & Astronomy, Macalester College, 1600 Grand Avenue, St. Paul, MN 55125

`jcannon@macalester.edu`

Andrew E. Dolphin

Raytheon Company, 1151 E Hermans Rd, Tucson, AZ 85756

`adolphin@raytheon.com`

Robert C. Kennicutt, Jr.

Institute of Astronomy, University of Cambridge, Madingley Road, Cambridge CB3 0HA, UK

`robk@ast.cam.ac.uk`

Janice Lee

Observatories of the Carnegie Institution of Washington, 813 Santa Barbara Street, Pasadena, CA 91101, Hubble Fellow

`jlee@obs.carnegiescience.edu`

Fabian Walter

Max-Planck-Institut für Astronomie, Königstuhl 17, D-69117 Heidelberg, Germany

`walter@mpia.de`

ABSTRACT

We use deep HST/ACS F555W and F814W photometry of resolved stars in the M81 Group dwarf irregular galaxy Ho II to study the hypothesis that the holes identified in the neutral ISM (HI) are created by stellar feedback. From the deep photometry, we construct color-magnitude diagrams (CMDs) and measure the star formation histories (SFHs) for stars contained in HI holes from two independent holes catalogs, as well as select control fields, i.e., similar sized regions that span a range of HI column densities. The CMDs reveal young (< 200 Myr) stellar populations inside all HI holes, which contain very few bright OB stars with ages less than 10 Myr, indicating they are not reliable tracers of HI hole locations while the recent SFHs confirm multiple episodes of star formation within most holes. Converting the recent SFHs into stellar feedback energies, we find that enough energy has been generated to have created all holes. However, the required energy is not always produced over a time scale that is less than the estimated kinematic age of the hole. A similar analysis of stars in the control fields finds that the stellar populations of the control fields and HI holes are statistically indistinguishable. However, because we are only sensitive to holes ~ 100 pc in diameter, we cannot tell if there are smaller holes inside the control fields. The combination of the CMDs, recent SFHs, and locations of young stars shows that the stellar populations inside HI holes are not coherent, single-aged, stellar clusters, as previously suggested, but rather multi-age populations distributed across each hole. From a comparison of the modeled and observed integrated magnitudes, and the locations and energetics of stars inside of HI holes, we propose a potential new model: a viable mechanism for creating the observed HI holes in Ho II is stellar feedback from multiple generations of SF spread out over tens or hundreds of Myr, and thus, the concept of an age for an HI hole is intrinsically ambiguous. For HI holes in the outer parts of Ho II, located beyond the HST/ACS coverage, we use Monte Carlo simulations of expected stellar populations to show that low level SF could provide the energy necessary to form these holes. Applying the same method to the SMC, we find that the holes that appear to be void of stars could have formed via stellar feedback from low level SF. We further find that Hα and 24μm emission, tracers of the most recent star formation, do not correlate well with the positions of the HI holes. However, UV emission, which traces star formation over roughly the last 100 Myr, shows a much better correlation with the locations of the HI holes.

Subject headings: galaxies: dwarf — galaxies: irregular — galaxies: individual (Ho II) — galaxies: ISM — stars: formation

1. Introduction

The role of star formation (SF) in creating structure and shaping the interstellar medium (ISM) is an important but unresolved topic. Studies of the neutral hydrogen (HI) component in a wide variety of nearby galaxies, including our own, reveal numerous holes, shells, and bubbles (for simplicity, we will refer to all types as holes throughout the paper), which span a great range in size and age (e.g., Heiles 1979; Brinks & Bajaja 1986; Puche et al. 1992; Oey & Massey 1995; Kim et al. 1999; Walter & Brinks 1999; Muller et al. 2003; Relaño et al. 2007; Chu 2008; Bagetakos et al. 2009). The origin of these ISM features has long been attributed to stellar feedback from massive stars, i.e., stellar winds and Type II supernovae (SNe) (Weaver et al. 1977; Cash et al. 1980; McCray & Kafatos 1987; Tenorio-Tagle & Bodenheimer 1988, and references therein). Typical ages of these ISM features, measured from the hole diameters and HI expansion velocities, range from $\sim 10^6 - 10^8$ yr (e.g., Oey & Massey 1995; Walter & Brinks 1999; Hatzidimitriou et al. 2005), which suggests that even if massive O and B type stars, the primary contributors to stellar feedback, are no longer present inside the HI holes, we should still see remnant stellar populations (assuming a universal IMF).

While the stellar feedback hypothesis of HI hole creation is appealing due to its intuitive simplicity, observational and theoretical studies do not provide much supporting evidence. The close proximity of dwarf galaxies in the Local Group (LG) has permitted detailed studies of correlation between stars and HI holes. In the LMC, Kim et al. (1999) compared the positions of 103 giant or supergiant HI shells with Hα, and found a weaker correlation than expected given the young ages of the shells. Similarly, Book et al. (2008) find that while Hα traces sites of secondary triggered SF around supergiant HI shells in the LMC, it is not exclusively associated with stars interior to the holes. Hatzidimitriou et al. (2005) cross-correlated the locations of 509 HI holes in the SMC with known catalogs of OB associations, supergiants, Cepheids, Wolf-Rayet (WR) stars, SN remnants, and stars clusters, finding 59 HI shells with no stellar component, and that holes without associated OB stars exceed those with them by factor of ~ 1.5. Further, in the LG dwarf irregular galaxy (dI) IC 1613, Silich et al. (2006) find that even the HI structures that do contain young stars do not have the observed properties consistent with the traditional stellar feedback theory.

The studies of the origins of HI holes in galaxies beyond the LG show similarly mixed results when testing the stellar feedback hypothesis. In the pioneering study of M31, Brinks & Bajaja (1986) found a strong correlation between OB associations and HI shells smaller than ~ 300 pc. Correlating high resolution HI imaging of the M81 Group dI Holmberg II with Hα, Puche et al. (1992) found strong evidence for a stellar feedback origin to the 51 HI holes. In a follow up study of Ho II, Rhode et al. (1999) used integrated BVR photometry to search for stars within the HI holes and found only 14% had a stellar component. A third study of Ho II concludes that Hα does not adequately trace the progenitor stellar populations; however, detected FUV emission associated with HI holes supports the stellar feedback model (Stewart et al. 2000). In another M81 Group dI, IC 2574, Pasquali et al.

(2008) use integrated colors from imaging from the Large Binocular Telescope to show that there is not a one to one correspondence between stars and HI holes, while an evaluation of alternative models by Sánchez-Salcedo (2002) finds that HI holes in IC 2574 are likely formed by stellar feedback.

Although a number of studies of select individual holes have found associated young stars (e.g., Oey & Massey 1995; van der Hulst 1996; Weisz et al. 2009), the overall evidence for a stellar feedback origin for all HI holes is not as compelling and a variety of alternate explanations have been proposed. For example, gamma ray bursts (GRBs) have sufficient energy to create holes in the HI without leaving a remnant stellar cluster (e.g., Loeb & Perna 1998). Similarly, collisions between high velocity HI clouds and a galaxy (e.g., Tenorio-Tagle et al. 1986) or ram pressure stripping from the intergalactic medium (e.g., Bureau et al. 2004) could provide the means to create observed ISM features. Rhode et al. (1999) suggest that modified energetics, either by an overestimation in the energies necessary to evacuate HI holes or by a non-standard IMF, could explain the observed discrepancies, although they acknowledge the latter is not likely. An alternate possibility is that gravitational instabilities and/or turbulence naturally give rise to structure in the ISM (e.g., Elmegreen 1997; Dib & Burkert 2005). The study of Constellation III by Harris & Zaritsky (2004) has cast doubt upon a number of these alternate theories and favors structure creation by numerous SF events. While it is likely that many of these mechanisms play a role in shaping the ISM at some level, quantifying the impact of stellar feedback on the ISM can give key insights into the feedback processes and self-regulation of SF.

A further alternative is that the traditional theory linking stellar feedback to the creation of HI holes is not complete. Specifically, the most rigorous observational test of the stellar feedback model (Rhode et al. 1999) assumed that single age stellar clusters generated the SNe energy necessary to evacuate the HI holes. This is a reasonable assumption based on an extrapolation from the theoretical models of the explosion and expansion of a single SN in the ISM (e.g., Chevalier 1974; Weaver et al. 1977). In this scenario, SNe from a single generation of stars (i.e., a cluster) explode, releasing energy into to an isotropic ISM, thus creating the observed hole and quenching future SF, by sweeping up and heating of the gas interior to the hole. However, the study of spatially resolved SFHs in nearby dwarf galaxies has provided evidence that SF within $\sim$ 500 Myr can return to the same locations (Dohm-Palmer et al. 1997; Dohm-Palmer & Skillman 2002; Weisz et al. 2009), demonstrating the SF does not always suppress subsequent generations of SF. The creation of HI holes by multiple generations of SNe is a scenario that would likely have complicated dynamics, but preserves the intuitive simplicity linking the energy production of stars with the structures in the ISM.

In this paper, we use HST/ACS imaging of Ho II to detect and study the resolved stellar populations within the HI holes independently catalogued by Puche et al. (1992) and The HI Nearby Galaxy Survey (THINGS; Walter et al. 2008; Bagetakos et al. 2009). Nearby dIs, such as Ho II (roughly a solid body rotator in the inner 2 kpc; Puche et al. 1992), are excellent environments for both the study of resolved stars and ISM features. Because the HI disks of dIs are typically solid body rotators, and thus lack sheer and differential rotation, HI holes and potential progenitor stellar components travel in unison for time scales on order of $\sim 10^8$ yr (e.g., Skillman et al. 1988; Skillman 1996). Further, the low metallicities of nearby dIs minimize internal extinction effects, which allow us to take a precise census of individual stars.

From the resolved stellar populations of Ho II, we construct color-magnitude diagrams (CMDs) and measure star formation histories (SFHs) corresponding to catalogued HI holes that fall into our ACS field of view. Using the SFHs we can compute the energy associated with stellar feedback and compare it to the energy required to evacuate an HI hole, allowing us to quantify the efficiency of stellar feedback and compare it to predictions from models. We further compare the stellar populations of the HI holes to those of select control fields, similar in size to the HI holes, which span a wide range in HI surface density and do not overlap with catalogued HI holes. The resolved stellar populations also permit us to directly test the conclusions of previous studies of Ho II by Puche et al. (1992) and Rhode et al. (1999), including comparisons to Hα, 24μm, and UV imaging of the same regions. Using the results of the stellar populations in the HI holes located within the ACS field of view, we use simulated CMDs to demonstrate the plausibility of HI hole creation due to stellar feedback in regions of low gas and stellar densities, such as the outer regions of galaxies. We then apply this method of analysis to the SMC and discuss how observations of apparently empty holes does not rule out the possibility of a stellar feedback origin.

2. Observations and Photometry

As part of a larger HST program aimed at imaging multiple dIs in the M81 Group (GO-10605), we observed Ho II on 2006, December 30 using HST/ACS (Ford et al. 1998). To capture most of the optical galaxy, we used two ACS fields, observing each field for 4660 sec in F555W (V) and 4660 sec in F814W (I), with a CR-split in order to reduce the impact of cosmic rays, and a dithering strategy to cover the chip gap. The images were processed with the HST pipeline and we performed photometry and artificial star tests using DOLPHOT, a version of HSTphot (Dolphin 2000) optimized for ACS observations[1]. Photometry was carried out as part of a larger program and the specific details, e.g., rejection criteria, completeness, can be found in Weisz et al. (2008). Following the photometric cuts, we merged the two fields into a single photometric list, appropriately removing duplicate stars, resulting in a total of 388,945 well measured stars for the combined fields. The deep photometry that is used in this paper has a limiting magnitude of $M_V \sim 0$, which allows us to see main sequence stars (MS) up to $\sim$ 300 Myr and Blue Helium Burning stars (BHeBs) up to $\sim$ 1 Gyr in age (Gallart et al. 2005; Weisz et al. 2008). To quantify the accuracy of the photometry we ran artificial star tests on the entire galaxy and found 50% completeness limits of $m_{F555W} = 27.8$ ($M_{F555W} = +0.15$) and $m_{F814W} = 27.3$ ($M_{F814W} = -0.15$), assuming a distance modulus of 27.65 (Karachentsev et al. 2002). A number of HI holes in nearby galaxies have inferred kinematic ages (from HI observations) as old as a $\sim 10^8$ yr (e.g., Puche et al. 1992; Walter & Brinks 1999). If some of the older HI holes were created by SF on this time scale, only deep photometry of resolved stellar populations would probe faint enough limits to detect the remaining stars.

---

[1] Photometry and artificial star tests for the HST/ACS imaging of Ho II is available via the ACS Nearby Galaxy Survey Treasury program (ANGST; Dalcanton et al. 2009): http://www.nearbygalaxies.org

The HI image we used in our analysis (panel (a) of Figure 1) was observed with the VLA using the B, C, D configurations in 1990 and 1991 (the full details of the observations are available in Puche et al. 1992). As part of the THINGS program (Walter et al. 2008), the observations were reprocessed with their software pipeline, achieving a final spatial resolution of $\sim 6''$ and a velocity resolution of 2.6 km s^{-1}. Both P92 and the THINGS team independently constructed catalogs of HI holes in Ho II by examining them in the position-velocity (pV) cuts and radius-velocity space in the HI data cube. Hole identification was done by eye using the following criteria as a guide: presence of the hole with a stationary center in multiple channel maps, sufficient contrast between the hole and its immediate surroundings, and the shape of the hole in radius-velocity space must be described by an ellipse (Puche et al. 1992; Bagetakos et al. 2009). Both catalogs contain the locations, diameters, expansion velocities of each of the holes (see Tables 1 $-$ 4 and Figure 1). Additionally, the THINGS catalog classifies each hole such that a type 1 hole has completely blown out of the disk of the galaxy, i.e, a break in the pV diagram, a type 2 hole only shows an approaching or receding side, and a type 3 hole has both sides present in pV space. While the P92 and THINGS holes catalogs are generally similar, the sizes, locations, and measured expansion velocities are not identical. For example, the THINGS catalog assigns an expansion velocity of 7 km s^{-1}to any blown out hole, while P92 lists expansion velocities for each hole, and does not indicate a blow out. Because of the high stellar density, slight differences in the hole locations and size can lead to different stellar populations. We explore this further in §4.3.

With a distance of 3.40 Mpc, measured from the tip of the red giant branch (Karachentsev et al. 2002), the high spatial resolution of HST/ACS (1 pixel = $0.05''$; $1'' \sim 16.5$ pc) allows us to probe scales much smaller than the minimum detectable HI hole size ($\sim$ 100 pc). Treating each hole as circular and using the central coordinates and diameters from each hole catalog, we overlaid these apertures over the HST/ACS drizzled image and found that 23 of the 51 holes from P92 and 19 of the 39 THINGS holes were within ACS coverage (Figure 2). In the P92 catalog, a portion of holes 10, 21, 25, 34, and 48 are outside our ACS field of view. We included those that primarily overlapped with the ACS data (10, 21, and 48), but excluded the others from the sample (25 and 34). From the THINGS catalog, we excluded holes 18 and 38 for the same reason. For consistency we used the HI hole numbering systems presented in the P92 and THINGS catalogs. Additionally, we selected nine control fields, regions in comparable size to the HI holes that do not overlap cataloged HI holes and span a range in HI column densities, and number them c1 − c9 (Figures 1 and 2).

3. Stellar Components of HI holes in Ho II

3.1. Luminous Main Sequence Stars Within the HI Holes

From our photometry we constructed CMDs of the stars in each of the 23 holes in the P92 catalog, 19 holes in the THINGS catalog, and nine control fields (Figures 3 − 6 and Tables 1, 2, & 5). Notably, we found that all holes in both catalogs contain a significant number of young stars; enough to easily identify CMD features by visual inspection and compare with the models of Marigo et al. (2008) (see Figure 7). However, these CMDs are not consistent with the expected CMD for a single age stellar cluster. The holes also have red giant (RGB) and asymptotic giant branch (AGB) stars with ages < 1 Gyr, as expected given that the older stars are fairly smoothly distributed throughout the optical galaxy (see Figure 11 in Weisz et al. 2008).

Young stellar clusters (e.g., OB associations) are traditionally associated with the formation of HI holes (e.g., Brinks & Bajaja 1986; Hatzidimitriou et al. 2005), and we tested this notion by making a census of the youngest and brightest stars. We identified young stars based on the stellar evolution models of Marigo et al. (2008), which suggest that the brightest 10 Myr old MS star at its turnoff has $M_{F555W} \sim -5$, or $m_{F555W} \sim 22.65$ in Ho II. We found 302 MS stars with $m_{F555W} < 22.65$ that also lay within holes in the P92 catalog. Further, restricting the color to be less than 0.05, i.e., $m_{F555W} - m_{F814W} < 0.05$, (to exclude Red Helium Burning stars (RHeBs), bright foreground stars, and most BHeBs) we find 109 stars that match our criteria. Of these 109 stars, 21 of them belong to hole 21, which is the largest and most populated hole with a diameter of ~ 2 kpc and $\sim 40{,}000$ stars in the CMD. Applying the above criteria for luminous MS stars to the remaining 21 holes, we found that all the holes have fewer than 10 bright MS stars and 20 holes have fewer than two bright MS stars. Similarly for the HI holes in the THINGS catalog, we found 347 stars with $m_{F555W} < 22.65$, and 104 stars with $m_{F555W} < 22.65$ and $m_{F555W} - m_{F814W} < 0.05$. Of these 104 stars, 30 belong to the largest hole (number 17). The other 18 holes all have fewer than 10 young MS stars, and 13 have fewer than two young MS stars. For the stars located in the control fields (Figure 6), we found that 32 match the bright MS star criteria, with c7 containing 21 of these stars, and six of the nine control fields containing two or less bright MS stars. The control field have more bright MS stars by a factor of ~ 1.5 when compared to the HI holes. We explore the impact of small number statistics, stochastic effects on the SFR, and production of massive stars in §5.

From these basic calculations, it seems that the location of young OB type stars are not a reliable tracer of the locations of HI holes, nor do they accurately represent the presence of young remnant stellar populations inside HI holes. We will discuss the spatial distribution of these stars further in §5.2.

3.2. The SFHs of Stars Within the HI Holes

Upper MS stars and BHeBs offer the opportunity to age date stellar populations more than 10 Myr old. To extract a more complete picture of the recent SF within the HI holes, we measured the SFHs for the stars inside each HI hole and compared the timing of SF activity to the inferred kinematic ages, i.e., the radius of the hole divided by its expansion velocity. We derived the SFHs, from the CMDs, using SFH recovery code of Dolphin (2002). This method constructs synthetic CMDs, using the stellar evolution models of Marigo et al. (2008), and compares them to the observed CMD using a maximum likelihood technique. To obtain this solution, we used a combination of fixed (e.g, binary fraction, IMF) and searchable (e.g., distance, extinction) parameters. We allowed the program to search for the best fit metallicity per time bin, with the condition that the metallicity must monotonically increase with time toward the present. We found the mean metallicity in the most recent time bins from the SFHs to be consistent with the observed value of $\sim 10\%\ Z_{\odot}$ (Miller & Hodge 1996), which is best fit by Z=0.002 isochrones (Figure 7). Throughout this paper, we use the following values when measuring SFHs or simulating CMDs: a standard power law IMF with $x = -2.3$ from 0.1 to 100 $M_{\odot}$, a binary fraction = 0.35, the stellar evolution models of Marigo et al. (2008), a distance of 3.40 Mpc, a foreground extinction of $A_{F555W} = 0.11$ (Schlegel et al. 1998), and 50% completeness limits of $m_{F555W} = 27.9$ and $m_{F814W} = 27.4$ (Weisz et al. 2008). To quantify the errors in the SFHs, we added the systematic uncertainties from the isochrones and the statistical uncertainties from Monte Carlo tests in quadrature. Quantifying the best fit solution and associated uncertainties from synthetic CMD matching has been subject to a number of extensive studies (e.g., Tosi et al. 1989; Tolstoy & Saha 1996; Gallart et al. 1996; Mighell 1997; Holtzman et al. 1999; Hernandez et al. 1999; Dolphin 2002; Ikuta & Arimoto 2002; Yuk & Lee 2007), which explore the nuances of this method beyond the scope of this paper. Full details on the method we used in this paper to measure the SFHs and quantify the associated errors can be found in Dolphin (2002).

As an example we present the observed, model, residual, and significance of the residual CMDs from the code of Dolphin (2002) for hole 23 in the THINGS catalog (Figure 8). Visual inspection of the observed and model CMD show broad agreement of features such as the young MS, BHeBs, RHeBs, and the RGB. The difference between the model and the observed CMD can been seen in the lower two panels, where black points indicate more real stars than synthetic stars, and white points indicating more synthetic than real stars. The residual significance diagram (panel (d)), reveals no distinct patterns of black or white points, indicating that the model CMD describes the data quite well.

We chose to focus on SF over the past 200 Myr in each of the holes (Figures 9 − 11) and control fields (Figure 12) based on the inferred kinematic ages of the holes derived from both hole catalogs. The time resolution of our SFHs is ∼ 10 Myr up to a look back time of 50 Myr and then ∼ 25 Myr from 50 − 200 Myr. These choices provide an adequate look back time and time resolution to see potential SF events responsible for the creation of the HI holes. Note that kinematic ages for HI holes are traditionally considered an upper limit to the age of the HI holes, as the expansion velocities were most likely higher in the past (e.g., Tenorio-Tagle & Bodenheimer 1988). We discuss the accuracy of inferred kinematic ages in more detail in §5.

As a check for accuracy of SFHs between the two hole catalogs, we compared the SFHs and CMDs from overlapping holes. The CMD of P92 hole 44 significantly overlaps with THINGS holes 26 and 31. The CMD of P92 hole 44 has 7566 stars, where as the two THINGS holes have 4253 and 3190, respectively. In terms of the SFHs, the peak SFR for P92 hole 44 occurs in the 40 − 50 Myr bin with a peak values of 5.6×10^{-3} $M_\odot$ yr^{-1}. Both the THINGS holes how peak SFRs in the same time bin, with values of 3.0×10^{-3} $M_\odot$ yr^{-1} and 3.2×10^{-3} $M_\odot$ yr^{-1}, or co-adding them, we find a peak SFR of $\sim 6.2\times10^{-3}$ $M_\odot$ yr^{-1}, consistent with the values for the single P92 hole. Similar tests were carried out for several other overlapping holes, and all were found to have consistent SFRs where expected. It is important to note that because the stellar density is not uniform in Ho II, even small differences in the location or radius of a hole, may result in significant differences in the stellar populations and SFHs.

We searched for differences between the stellar populations of the control fields and the HI holes by comparing their cumulative SFHs (i.e., fraction of stars formed as a function of time) over the past 14.1 Gyr (lifetime) and 200 Myr (recent) by performing a KS test comparing the average cumulative SFHs for the holes and control fields (red lines in Figure 13). As expected, the majority of the holes and control fields share a common old stellar population, i.e., at least 50% of the stars were formed greater than 6 Gyrs ago), and the fraction of stars formed in the last 6 Gyrs is also consistent between the hole and control field samples. Although the past 200 Myr is likely more influential when it comes to hole formation, again we see no discernible difference between the recent cumulative SFHs of the two samples. The KS test confirmed these impressions, indicating that, on both the lifetime and recent time scales, the stellar populations of the holes and control fields have the same parent distribution. From the perspective of the traditional stellar feedback hypothesis, this is an unanticipated result, as the theory would expect young stars associated with remnant clusters to be predominantly located inside the HI holes, and not control fields. This is discussed in more detail in §5.

4. Comparing the Energy from SF to the Energy Needed to Create an HI Hole

Quantifying the energy generated from SF and the energy necessary to create an HI hole is of particular importance in understanding the role stellar feedback plays in creating HI holes. Fortunately, the interaction of a single SN and the surrounding ISM has been modeled in great detail (e.g., Chevalier 1974; Weaver et al. 1977; Heiles 1979). In addition, energy associated with SF is computed by the galaxy evolution modeling code STARBURST99 (Leitherer et al. 1999). STARBURST99 takes a SFH as input and uses stellar evolution models to produce predictions for spectrophotometric, chemical, and stellar energy output properties of galaxies that have had episodes of SF within the last 1 Gyr. For the particular case of stellar feedback, STARBURST99 can compute the energy profiles (i.e., energy produced by stellar winds and SNe) using the SFHs for individual holes, which allows us to directly connect stellar feedback to the creation and evolution HI holes. In this section, we apply each of these methods to the HI holes in Ho II and their stellar populations, and compare them to expected stellar feedback efficiencies from a variety of hydrodynamical simulations.

4.1. Energy Required to Evacuate an HI Hole

The minimum amount of energy required to evacuate an HI hole is given by the single blast model of Chevalier (1974):

$$E_{Hole} = 5.3 \times 10^{43} \; n_0^{1.12} \; (\frac{d}{2})^{3.12} \; v^{1.4} \tag{1}$$

where E_{Hole} is in the units of 10^{50} ergs, n_0 is the HI volume density (cm^{-3}) at the mid-plane of the galaxy, d is the diameter of the HI hole in pc, and v is the expansion velocity in km s^{-1}. While the expansion velocity and diameter of the hole are independently measured quantities, n_0 is dependent upon the HI column density, N_{HI}, and scale height of the gas, h, in the following way:

$$n_0 = \frac{N_{HI}}{\sqrt{2\pi}h} \tag{2}$$

The denominator, $\sqrt{2\pi}h$ is the effective thickness of the gas assuming a Gaussian distribution, with h being the 1σ scale height.

One of the challenges in determining E_{Hole} is accurately measuring n_0. Both P92 and Bagetakos et al. (2009) use a rotation curve to estimate the total mass in a gravitationally bound spherical system. This value was averaged over the volume of a sphere with a radius,

$R_{V_{max}}$ and multiplied by a factor of two. Measuring $\sigma_v = 6.8$ km s^{-1}(HI velocity dispersion), P92 found $h = 625$ pc, and Bagetakos et al. (2009) find $h = 600$ pc. P92 used this method to compute the scale height of M31, and found it to be in agreement with the mass-model based method of Brinks & Burton (1984). However, P92 acknowledged that wide-field, deep photometry of Ho II, would produce an accurate mass model of Ho II, and a more precise knowledge of h, n_0, and E_{Hole}.

Fortunately, we had access to high quality 3.6μm imaging of Ho II through the Local Volume Legacy Survey (LVL; Lee et al. 2008; Dale et al. 2009) taken with the *Spitzer Space Telescope*, which allowed us to construct such a mass model. The LVL team provided a calibrated (including foreground star subtraction) 3.6μm image of Ho II. From this image, we used the ISOPHOT package in IRAF[2] to perform surface photometry, accounting for inclination and position angle effects ($i = 47°$, PA = 177°; Puche et al. 1992) starting at the dynamical center of the galaxy (α = 08:19:18, δ = +70:42:37; J2000), which yielded a surface brightness profile as a function of galactocentric radius (Figure 14). Following the method described in § 4 of Oh et al. (2008) and assuming the 3.6μm mass to light ratio, $\Gamma_\star$ = 0.5 (comparable to other dwarf irregulars; Walter et al. 2008), we converted the surface brightness profile into a surface mass density profile, Σ.

The isothermal gas scale height equation (Equation 3) derived by Kellman (1970) (and used by Kim et al. 1999 for the LMC) relates the surface mass density, Σ and the HI velocity dispersion, σ_v, to the HI scale height, h. For Ho II, Bureau & Carignan (2002) derived σ_v as a function of galactrocentric radius, allowing us to compute the HI scale height as a function of radius.

$$h = \frac{\langle\ \sigma_v^2 \rangle}{\pi G \Sigma} \tag{3}$$

We now have two independent estimates of the gas scale height, namely the HI scale height of P92 and that inferred from surface photometry. We found the HI scale height derived by P92 to be larger by a factor of $\sim 3-5$ in the innermost 2 kpc of the galaxy, and in agreement at $\sim$ 4 kpc. At radii larger than 2 kpc, h is in better agreement between the different methods.

We computed new values of n_0, as a function of radius, using Equation (2) along with the newly calculated HI scale height and the values of N_{HI} measured by P92. Because the P92 N_{HI} values showed multiple large fluctuations in the inner region of the galaxy, likely due to the presence a number of HI holes, we interpolated over the regions of large fluctuations to ensure a smooth, continuous distribution. Effectively, the largest difference in the P92 and new estimated values are due to the differences in the HI scales heights. The HI scale height derived from surface photometry effectively increases the values of n_0 by a factor of ~ 3 compared to the P92 and Bagetakos et al. (2009) values, which in turn increases E_{Hole} by approximately the same amount.

---

[2] IRAF is distributed by the National Optical Astronomy Observatory, which is operated by the Association of Universities for Research in Astronomy (AURA) under cooperative agreement with the National Science Foundation.

It is important to note that the values of E_{Hole} are likely lower limits on the energy necessary to evacuate an HI hole. The values of n_0 are the *average* HI volume density at a given radius. However, observationally, SF occurs at higher than average values of n_0, suggesting that to get a true sense of E_{Hole} we would need to measure a peak value of N_{HI} inside the HI holes. Although this is not observationally plausible, we can get a sense of how a larger values of N_{HI} would affect E_{Hole}. As an example, we examined control field 5, which is located near one of the highest regions of current SF in Ho II. From Equation (3) and the peak N_{HI} measured inside c5, we find an increase by a factor of ~ 8 in the the peak value of n_0 versus the average value. This translates into an increase in E_{Hole} by a factor of ~ 10, suggesting that E_{Hole} values present here are likely lower limits.

4.2. Energy Associated with Star Formation

A basic criteria of the stellar feedback model is that the energy associated with SF must exceed the energy necessary to evacuate a given HI hole. To calculate the available energy due to SF, we used the galaxy evolution modeling software STARBURST99 (Leitherer et al. 1999). We simulated a single instantaneous burst of SF with a fixed mass of 10^6 $M_\odot$using STARBURST99 parameters that matched those described in §3.2, including a metallicity of $Z = 0.002$, a SN cutoff mass of 8 $M_\odot$, and a time sampling of 5 Myr.

Because the energy output from STARBURST99 scales linearly with the input mass, we ran one simulation (with a stellar mass of 10^6 $M_\odot$), and then subsequently scaled it by the integrated stellar mass from the SFHs of stars inside each hole, sampled at 5 Myr intervals. The cumulative distribution of the energy generated from SF from the present ($t = 0$) to 200 Myr for the stars inside each HI hole are shown in Figures 15 − 20. The inferred kinematic ages are denoted by the grey dashed line, and efficiencies (see §4.3) of 100%, 10%, and 1% are indicated by the red, green, and blue dashed lines, respectively.

We have examined the efficiency over the inferred kinematic age for both catalogs as a function of galactrocentric radius, hole radius, expansion velocity, and inferred kinematic age (Figure 21). For both hole catalogs the clearest trend we found is that efficiency seems to increase with expansion velocity. However, this result is likely misleading, because of the differences in assigning expansion velocities. In the THINGS, catalog, if a hole was blown out, it was assigned an expansion velocity of 7 km s^{-1}, whereas P92 attempted to measure the best fit expansion velocity for each hole. Thus, if we assigned each P92 hole with an expansion velocity lower than 7 km s^{-1}, the value of 7 km s^{-1}, there would be no trend in the P92 sample, consistent with the THINGS sample. Based on the THINGS catalog classification (see §2) of hole types, we found that holes that have not blown out (type 2 or 3), tend to have efficiencies higher than expected from models (see §4.3 for a description of the models), in some cases exceeding 100%. In contrast, holes that have blown out generally fall within the expected range. Again, this trend is likely due to the measurement techniques of the HI expansion velocities. In general, a blown out hole has stalled expansion, and its expansion velocity is not detectable above the random HI motions. Thus, the measurements of E_{Hole} are highly uncertain for blown out holes as are the efficiencies. The underlying implication is that the creation of an HI hole is a complex event that cannot be accurately represented by a simple kinematic age or efficiency, rather a more complex model is necessary (see §5 for more discussion).

4.3. Comparing Energies and Feedback Efficiencies

We then compared the inferred energy from SF over the kinematic age of each hole, E_{SFKA}, to the energy needed to produce the observed properties of each hole, E_{Hole}. The ratio of E_{Hole} to E_{SFKA} allows us to calculate the a 'putative' stellar feedback efficiency, ϵ, over the inferred kinematic age of each hole (see Tables 3 and 4). Models of SF including feedback and interactions with the ISM expect such efficiencies to range from $\sim 1\% - 20\%$ (Theis et al. 1992; Cole et al. 1994; Padoan et al. 1997; Thornton et al. 1998). 15 of the 23 P92 holes and 6 of the 19 THINGS holes have putative efficiencies between $1 - 20\%$, in agreement with the models. Overall, a higher fraction of P92 holes are within the expected efficiency range than THINGS holes. While this may seem to be an unexpected result, this actually underlines the complexity of the connection between stars and HI holes. For example, P92 hole 42 and THINGS hole 27 are roughly the same size, but slightly different central coordinates, which results in the the THINGS hole having more stars in its CMD by a factor of ~ 2, in turn influencing the SFH and feedback efficiency. Of the holes that are not consistent with the expected range, one P92 hole (number 48) has an efficiency greater than 100%, while five THINGS holes (9, 12, 14, 23, 39) also have efficiencies greater than 100% (Figure 21). These outliers suggest that perhaps energy from stellar feedback is not sufficient to have created these holes.

For example, P92 hole 14 (Figure 15) has an efficiency of $\sim 1\%$ where the inferred kinematic age intersects the cumulative energy profile. In comparison, P92 hole 30 (Figure 16) has a kinematic age efficiency of 39%, outside the theoretical range predicted by models. Further, ratios that require $\epsilon > 100\%$ indicate that there has not been enough energy for SF during the inferred kinematic age of each hole. However, Figures $15 - 20$ show that there has been sufficient energy available during the most recent 200 Myr even in these extreme cases, suggesting that perhaps the inferred kinematic ages do not truly represent the ages of the holes, or that the concept of an HI hole age is intrinsically ambiguous for holes that contain multiple generations of stars.

To explore this possibility, instead of using the inferred kinematic age as a guide, we assumed a nominal 10% efficiency and recalculated the age of the hole to match the time scale needed to give sufficient energy input from SF. For example, while P92 hole 48 (Figure 17) has a kinematic age efficiency of 120%, the energy profile shows that over the past 200 Myr, enough energy was generated from SF to have created the hole, if the hole is $\sim$ 100 Myr old (assuming a nominal 10% efficiency). Similarly, for the other P92 and THINGS holes that have efficiencies outside the theoretical range, the same analysis shows that there is ample energy from SF to have created each of those holes in the past 200 Myr. We defined a 'look back age' as the time at which the line of 10% efficiency intersects the energy profiles in Figures 15 $-$ 20. We then compared the ratio of the look back age to the inferred kinematic age, and found that the inferred kinematic ages are generally lower than the look back times (Figure 22). While perhaps not the most rigorous definition of the age of a hole, the look back age suggests that the inferred kinematic age may not accurately represent the true age of HI holes, even as an upper limit. We explore the kinematic age discrepancy in greater detail in §5.

4.4. Connecting the Spatially Resolved Star Formation History to the HI Surface Density

In addition to the measuring the SFR as a function of time, we can use spatial information from the resolved stellar populations to qualitatively compare the location of SF episodes with HI column densities. Following a method of analysis similar to Dohm-Palmer et al. (1997), we used BHeBs from the entire HST/ACS CMD of Ho II (Weisz et al. 2008) and constructed movies of the spatially resolved recent SFH over the past $\sim$ 200 Myr. The initial masses of BHeBs range from $\sim 2 - 20$ $M_{\odot}$, giving them lifetimes between $\sim 5 - 500$ Myr. More importantly, BHeBs have a one-to-one correspondence between luminosity and age. BHeBs of a single age therefore occupy a *unique* location on a CMD, making them superb tracers of recent SF. In contrast, multiple generations of MS stars can occupy the same location on the CMD, making age dating of most individual MS stars from the CMD virtually impossible (see Dohm-Palmer et al. 1997; Gallart et al. 2005; Weisz et al. 2008, for a more in depth discussion of age dating stars from CMDs).

By measuring its magnitude, we can assign a unique age to each BHeB, using the models of stellar evolution. We can then trace the location of SF as a function of age based on BHeB positions in the ACS image. While it is true that many young star clusters dissolve into the field on time scales of $\sim$ 10 Myr (e.g., Lada & Lada 2003), the stars can maintain spatial coherence for much longer. Empirically, CMD-based studies of the SMC and LMC find that star forming structures (such as associations) can remain coherent for up to a couple hundred Myr (Gieles et al. 2008; Bastian et al. 2009).

We were able to isolate the BHeBs on the CMD by visual inspection because Ho II has a large number of BHeBs, and low foreground and internal reddening values. We constructed a smooth analytic function mapping the magnitudes of the BHeB track to unique ages, using the stellar evolution models of Marigo et al. (2008). Applying this function to the observed BHeBs, we assigned each star an individual age, with an uncertainty of $\lesssim$ 20%. We created density maps of the BHeBs by placing the stars into 5 Myr bins and converting their x and y coordinates to RA and Dec. We then smoothed the resulting images with a Gaussian kernel with a FWHM $\sim 15''$.

To convert the BHeB density maps (stars pixel^{-1}) to SFR/area (M$_\odot$ yr^{-1} kpc^{-2}), we first divided each frame (i.e., 5 Myr binned density maps) by the sum of the pixel values to determine the fractional contribution of each pixel to the total stellar density in each frame. That is, if a normalized pixel had a value of 0 it did not contribute to the SF in the frame, while a pixel with a value of 0.01 contributed to 1% of the SF in that frame. The density maps were then connected to the SFH of the field (Weisz et al. 2008).

First, we re-binned the SFH with different time resolutions: 10 Myr for a look back time of $\sim$ 100 Myr and 20 Myr for a look back time of $\sim$ 200 Myr, in order to match the decreasing time resolution at older ages. We then interpolated each to a 5 Myr time sampling to match the temporal resolution of the stellar density maps. We then multiplied each stellar density map by the corresponding SFR and divided by the physical area of the ACS field of view, thus converting the images from units of stars pixel^{-1} to SFR/area. We then performed bilinear interpolation over time and space to ensure smooth and continuous movies. The result is two movies of the spatially resolved SFHs of Ho II with units of SFR/area, with look back times of $\sim$ 100 and $\sim$ 200 Myr, and a spatial resolution of $\sim 15''$ ($\sim$ 250 pc). Figures 23 and 24 show select still frames of the two movies with HI contours overlaid.

The general trends presented by the spatially resolved SFHs are that low level SF has dominated the galaxy in the most recent $\sim$ 200 Myr, with only a substantial rise in the SF activity in the last $\sim$ 40 Myr. The smoothness of the SFH implies that the HI holes were not produced by a series of intense episodes of SF, instead the holes were created due to low level SF with some variation above a constant value, which has steadily input energy into the ISM. As a comparison, we integrated the spatial resolved SFH of the region corresponding to THINGS hole 17 and found general agreement between the two. For example, both SFHs show a peak at $\sim$ 40 Myr, and from the integration of the spatially resolved SFH we found the SFR at this time to be 3.0×10^{-2} M$_\odot$ yr^{-1}, whereas the SFH from Figure 5 shows a SFR of 4.0×10^{-2} M$_\odot$ yr^{-1}. While this difference of 30% may seem large, in fact, the systematic and statistical uncertainties from the two methods are $\sim$ 20% from the temporal SFH and 50% from the spatial SFH, which implies these are consistent values.

These movies allow us to investigate the correlation between HI density and SF on different time scales. Within the last $\sim$ 40 Myr, the SF is well correlated with high HI surface density, as has been seen in Hα, and UV imaging (see §5.2 for a discussion on Hα and UV imaging). On longer timescales, we note that the SF patterns do not adhere to the locations of high HI column densities. In particular, there is a relatively high level of SF activity in the large HI void, corresponding to P92 hole 21 and THINGS hole 17, $\sim$ 40 Myr ago, which has been preceded by low level activity for at least the past $\sim$ 200 Myr.

5. Discussion

5.1. The Paradoxical Results of Rhode et al. (1999)

The study of Ho II by Rhode et al. (1999) is perhaps one of the most rigorous observational tests of the stellar feedback model of HI hole creation. Despite the appeal of the stellar feedback theory of HI hole formation, Rhode et al. (1999) found no compelling evidence supporting this hypothesis, and their conclusions seriously challenged the standard model of HI hole formation. The non-detection of stars in the majority of HI holes contradicted expectations for stellar feedback as a universal mechanism of hole creation, although Rhode et al. (1999) did not rule out stellar feedback as the source of small HI holes in the central regions of Ho II.

Rhode et al. (1999) searched for single age stellar clusters, but likely did not find them because the single age cluster model can overestimate the surface brightness of the remnant stars by a significant amount, for a variety of reasons we explore in the following sections. Further, using only integrated light, it can be difficult to distinguish between a single age stellar cluster and a mixed age stellar population, which can make it difficult to age date stars that are detected. As a comparative test, we computed the integrated magnitudes of each of the Rhode et al. (1999) apertures from the HST/ACS CMDs. Our integrated photometry is in agreement with that of Rhode et al. (1999). A histogram of the resulting integrated magnitudes reveals that the six regions where Rhode et al. (1999) did detect stars are among the brightest in the sample (Figure 27). The rest of the regions were classified as non-detections, despite containing significant numbers of young stars.

Using the HST/ACS photometry of Ho II we constructed CMDs of the apertures (panel (d) of Figure 1 and Table 6) defined by Rhode et al. (1999). Figures 25 and 26 unequivocally show well-populated CMDs of mixed age stellar populations, including young MS stars and HeBs, which are likely the remnant stars Rhode et al. (1999) attempted to detect using integrated light. Our interpretation is that single age stellar populations do not produce a majority of the HI holes in Ho II, confirming the conclusions of Rhode et al. (1999).

5.2. A New Model

Instead of assuming that a single age cluster was responsible for the creation of HI holes, we explored the possibility that a mixed age stellar population producing SNe tens or hundreds of Myr apart was responsible for the creation of HI holes. Specifically, we asked how a remnant mixed age stellar population would differ from a single age cluster in terms of the integrated light properties, location of stars inside HI holes, and energetics associated with this different mode of SF.

To illustrate this, we generated synthetic CMDs, with the same parameters (e.g., IMF, binary fraction, distance, etc.) used to measure the SFHs in §2.2, and computed the mean expected integrated magnitudes of different stellar populations. To ensure that we were not in a regime where stochastic effects are important, we fixed the integrated mass of the simulations to be 10^6 M$_\odot$, $\sim$ 1% of the stellar mass of Ho II and at least a factor of 100 greater than the stellar mass within any given hole. We limited the simulations to the most recent 100 Myr, the approximate age regime of the majority of HI holes in Ho II. The simulations were run 100 times, which produced an average statistical error of $\sim$ 0.01 mags. Effects of completeness and photometric error are similarly $\sim$ 0.01 mags. Neither source of error has a large impact on the results at magnitudes this bright.

The first model assumed that all the stellar mass was formed in a $\sim$ 5 Myr period 50 Myr ago, with no subsequent SF. For this, 'burst' model, we found the mean integrated magnitude and color to be m$_{F555W}$ = 15.88 and m$_{F555W}$ $-$ m$_{F814W}$ = 0.48. For comparison, we distributed the same integrated stellar mass with a constant SFR over the period of 50 $-$ 100 Myr and found m$_{F555W}$ = 16.07 and m$_{F555W}$ $-$ m$_{F814W}$ = 0.51.

We further considered a two component SFH model. We distributed 10^6 M$_\odot$ in stellar mass with a constant SFR from 50 $-$ 90 Myr ago, no SF from 35 $-$ 50 Myr ago, constant SFR from 25 $-$ 35 Myr ago, and quiescence for the most recent 25 Myr. This multiple episode model produced stars with integrated properties of m$_{F555W}$ = 15.86 and m$_{F555W}$ $-$ m$_{F814W}$ = 0.54. Comparing the single age, constant, and multiple episode models of the same integrated stellar mass, we found they produced results that were indistinguishable in terms of integrated light.

To illustrate this point empirically, we compared the stellar populations of P92 holes 42 and 43, which both have integrated magnitudes of m$_{F555W}$ = 18.75, but differ in other properties. For example, hole 42 contains 1383 stars and has an inferred kinematic age of 17 Myr, but hole 43 has 549 stars and an inferred kinematic age of 26 Myr. The SFHs of stars within the two holes differ significantly in the last 10 Myr. SF in hole 42 had been more prominent $>$ 10 Myr ago, however within the last 10 Myr, hole 43 has a higher SFR, likely producing young bright stars that dominate the integrated light of the stellar population. These findings suggest that integrated light can only serve as an indicator of recent SF, but cannot give an accurate account of the SFH.

The dissolution of stellar clusters into the field further complicates integrated light observations and analysis of clusters. Lada & Lada (2003) note that the most common stellar clusters contain only dozens of stars and disperse into the field within $\sim$ 10 Myr, which is the so-called 'infant mortality' scenario of cluster dissolution. Detailed studies of structure of stellar groups in the SMC and LMC show that only $\sim 3 - 7\%$ of young stars survive in clusters past the age of ~ 10 Myr (Gieles et al. 2008; Bastian et al. 2009). Applying this idea to Ho II, it suggests that the remnant stellar populations would not be highly clustered, but instead would be distributed across the HI hole, resulting in fainter integrated magnitudes than expected for clustered stars. To look for this effect we selected MS stars from the HST/ACS photometry by applying magnitude and color restrictions that isolated young MS stars (< 10 Myr (red) and < 75 Myr (blue)) and plotted their positions relative to the HI holes catalogs, Rhode et al. (1999) apertures, and control fields (Figure 28). While there is some clustering of young stars, particularly those < 10 Myr in age, the clusters of stars are typically on the edges of the HI holes where triggered secondary SF due to the expansion of the hole is likely taking place (e.g., Tenorio-Tagle & Bodenheimer 1988). The majority of the MS stars < 75 Myr in age are not clustered, which makes the integrated light of these stellar populations appear fainter than had they been bound or appeared as unresolved stellar clusters.

One of the most interesting cases presented by Rhode et al. (1999) is that of P92 hole 10. Based on its HI properties at least several dozen SNe would be necessary to have created hole 10. The remnant stars from a burst should be well above the detection criteria used by Rhode et al. (1999) in a single cluster model, but none were detected. Rhode et al. (1999) assumed a single remnant cluster would be in the center of the hole and used an aperture smaller than the hole to search for the stars. Comparing the CMD between the actual hole and the aperture shows why the stars likely responsible for creating hole 10 were not detected by Rhode et al. (1999). The CMD of the entire hole has ~ 4200 stars and an integrated magnitude of $m_{F555W} = 17.68$, while the CMD of the Rhode et al. (1999) hole 10 aperture contains 893 stars and has an integrated magnitude of $m_{F555W} = 19.75$. Furthermore, the spatial distribution of MS stars < 75 Myr in age (Figure 28) show that the photometric aperture of hole 10 has no stars, while the hole itself contains a number of young stars. It appears that the bright stars either did not form centrally in hole 10 or they have rapidly diffused out of the center, if they did form there. Although this hole was considered among the strongest evidence against the stellar feedback theory of HI hole creation, it now only seems to confirm that the single age cluster model of hole formation is not the appropriate mechanism for HI hole creation.

If HI holes form via multiple generations of SNe, understanding the underlying physics becomes more complicated. We have to go beyond the simple single blast model of HI hole creation and consider the complex interplay between the local ISM and stellar feedback, which seems to be the dominant mechanism behind structure formation in the ISM (e.g., Harris & Zaritsky 2008). Heiles (1990) considers the case of ‘clusters of clusters’ of SNe present within an HI hole, noting that sequential explosions would contribute to the mechanical energy expanding the hole as well as significantly alter the gas density inside the hole. Oey & Clarke (1997) also conclude that multiple OB associations would increase the mechanical power and time scale of energy input into expanding the shell. Recchi & Hensler

(2006) present a model demonstrating how two separate SF events inside an HI hole would delay the onset of the hole refilling with cold gas with time scales from $\sim 100 - 600$ Myr depending on local conditions, indicating the multiple episodes of SF spread out over time can help extend the life of an HI hole. Projection effects could cause generations of stars along a line of site appear to be spatially co-incident within a given HI hole. However, this is likely a small effect because the disk-like nature of Ho II implies that the stellar scale height is much less than that of the HI, suggesting a reasonable assumption is that the young stars are primarily located in the mid-plane of the disk.

Quantitative modeling of the impact of the complex scenarios presented by multiple generations of SF inside HI holes has yet to be carried out in detail. Presently, the single blast approximation and kinematic age estimations of HI holes are dependent upon quantities (e.g., expansion velocity, volume density) that likely have varied over the history of a given hole. Quantifying the precise impact of these parameters on HI hole formation and energetics is beyond the scope of this paper. For example, while why control fields and HI holes contain similar stellar populations, but vastly different HI column densities, is an open question. However, Ho II may not be the best galaxy to answer this question, because we are not sensitive to HI hole smaller than $\sim$ 100 pc. Thus, if it is the case that larger holes are mergers of multiple smaller holes, we simply may not be sensitive to the small holes forming inside the control fields. Analysis similar to that presented in this paper using galaxies with smaller resolvable HI holes (e.g., LMC or SMC) along with computer modeling that accounts for the effects of an anisotropic ISM and multiple generations of SNe could lend insight into the fundamental physical processes that are responsible for shaping the ISM and driving HI hole formation.

5.3. HI Holes in the Outer Regions of Ho II

Of particular interest to Rhode et al. (1999) are the presence of HI holes outside the the optical body of the galaxy. While they do not rule out the possibility that the inner holes could have formed from SF, the typical HI densities in the outer regions of Ho II are relatively low, which is not very conducive to SF (Kennicutt 1989). However, the properties of holes in outer regions of galaxies do not differ from those in inner regions (Brinks & Bajaja 1986; Puche et al. 1992; Hatzidimitriou et al. 2005; Bagetakos et al. 2009), suggesting that the same underlying mechanism, namely stellar feedback, is responsible for HI holes in both environments. To this end, we used a Monte Carlo method to compute expected stellar populations in the outer holes of Ho II to see if their creation via stellar feedback is possible.

From E_{Hole} we can calculate the SFR over the kinematic age, SFR_{KA}, for a typical outer HI hole and then use it to construct simulated CMDs to determine properties of the expected stellar populations. We find that the 19 holes from Bagetakos et al. (2009) located outside our ACS coverage have a mean diameter $\sim$ 800 pc, an expansion velocity ~ 8 km s^{-1}, a kinematic age $\sim$ 50 Myr, an HI volume density of 0.1 cm^{-3}, and $E_{Hole} \sim 100 \times 10^{50}$ erg. Assuming 10^{51} erg per SN (McCray & Kafatos 1987) and that 10% of this energy goes into moving the ISM (Theis et al. 1992; Cole et al. 1994; Padoan et al. 1997; Thornton et al. 1998), $\sim$ 100 SN are needed to create an HI hole with these properties, equivalent to a SN rate over the kinematic age of $\sim 10^{-6}$ SN yr^{-1}. Assuming that the SNe come from stars with M $>$ 8 M$_{\odot}$, we find SFR$_{KA} \sim 2\times10^{-5}$ M$_{\odot}$ yr^{-1} for all stars, using our standard IMF (§3.2). This SFR implies an integrated stellar mass of $\sim 10^3$ M$_{\odot}$ over the kinematic age.

With this SFR as input, we constructed simulated CMDs, via a Monte Carlo process using either a constant or a burst model. The input for the constant SFR model had a SFR = 2×10^{-5} M$_{\odot}$ yr^{-1} from 50 Myr to 100 Myr. This focuses on the brightest stars and most recent SF likely to have created the HI hole. The burst model assumed a burst of SF 50 Myr ago, producing 1000 M$_{\odot}$. We ran each simulation 100 times to account for the statistical fluctuations. For the constant model, we find that the average CMD of the remnant stars has $\sim$ 7 stars and an integrated magnitude of m$_{F555W}$ = 24.00, assuming a limiting photometric depth equal to the 50% completeness limit (Weisz et al. 2008). For the burst model, the average CMD of the remnant stars had $\sim$ 8 stars and a integrated magnitude of m$_{F555W}$ = 23.75. Both cases results in integrated magnitudes fainter than the predictions by Rhode et al. (1999) as well as the hole and control fields presented in this paper. The remnant stellar populations in the outer holes are likely only detectable with deep photometry of resolved stars.

Other common methods of searching for stellar populations inside HI holes include the use of Hα, 24μm, and UV imaging (e.g., Puche et al. 1992; Stewart et al. 2000; Muller et al. 2003). UV traces a stellar population with initial masses $\gtrsim$ 3 M$_{\odot}$ and time scales of $\sim$ 100 Myr, while Hα (and 24μm in more dusty environments) traces ionizing photons from MS stars with initial masses of $\gtrsim$ 20 M$_{\odot}$ and ages $\lesssim$ 10 Myr (see Kennicutt 1998, for a full review of different SFR indicators and their properties). A number of studies aimed at testing the stellar feedback theory of hole creation via this type of imaging have have done so with a mixed degree of success (Puche et al. 1992; Kim et al. 1999; Rhode et al. 1999; Stewart et al. 2000; Muller et al. 2003; Cannon et al. 2005; Book et al. 2008). Given the low SFRs we have derived ($10^{-4} - 10^{-5}$ M$_{\odot}$ yr^{-1}) within many of the HI holes, it is not entirely surprising that these imaging techniques have yielded such mixed results. Simulations have shown that for SFRs below $\sim 10^{-4}$ M$_{\odot}$ yr^{-1} stochastic processes become important and Hα is no longer a reliable tracer of SF (Tremonti et al. 2007; Thilker et al. 2007; Meurer et al. 2009). Although a similar study in the UV has yet to be conducted, given the small number of stars expected in any given CMD, it is likely that the UV has a similar cut-off SFR. Indeed, Stewart et al. (2000) used FUV imaging of Ho II to show that there is some agreement between HI hole locations and bright UV regions, but did not find a good one to one correlation.

We can test for UV-bright stellar populations within the outer holes using data from the Local Volume Legacy sample (Lee et al. 2008; Dale et al. 2009), which contains FUV and NUV imaging originating from the GALEX Nearby Galaxies Survey (Gil de Paz et al. 2007), and the Hα and 24μm images from the Spitzer Infrared Nearby Galaxies Survey (SINGS Kennicutt et al. 2003). Overlaying the HI hole and Rhode et al. (1999) aperture locations over these images, we compared the location of bright regions with known HI holes (Figures 29 − 31). Because the correlation between low SFRs and Hα, 24μm, and UV is not well understood, we are only able to make qualitative conclusions. From all the images, it is evident that there is not a one to one correlation between any of these fluxes and the stellar populations inside the HI holes as shown in the HST/ACS based CMDs. This simple test demonstrates that deep photometry is necessary to understand the formation and histories of HI holes.

5.4. Comparison with the SMC and LMC

Perhaps the biggest challenge to the stellar feedback model of HI hole creation comes from observations of some of the closest galaxies. The proximity of the SMC and LMC allow for detailed observations, including high resolution HI imaging, which probes physical scales as small as $\sim$ 15 pc (Kim et al. 1999). Matching catalogs of young stellar objects (e.g., OB associations, supergiants, WR stars) and Hα imaging to HI hole catalogs, three recent studies of the LMC (Kim et al. 1999), the SMC (Hatzidimitriou et al. 2005), and the Magellanic Bridge (Muller et al. 2003) do not find strong correlations between the locations of young stellar objects and HI holes. The largest challenge to the stellar feedback creation hypothesis posed by these studies are the presence of young HI holes ($\sim 2-10$ Myr) with no associated young stellar objects (Stanimirović 2007). This is particularly problematic in the SMC, where Hatzidimitriou et al. (2005) identified 59 young holes ($\sim 5 - 10$ Myr) that appear to be void of young stellar objects. Hatzidimitriou et al. (2005) further find that the physical characteristics of these particular holes are no different than those with stellar components. Further, Hatzidimitriou et al. (2005) conclude that the properties of the HI holes in the inner and outer region are indistinguishable and that from their analysis there is no evidence to suspect a different creation mechanism for inner and outer holes.

Using the same type of analysis as in §5.3, and the assumption that inner and outer holes are indistinguishable in their HI properties Hatzidimitriou et al. (2005), we can compute the properties of the expected stellar populations if these young holes were formed due to stellar feedback. For the 59 empty HI holes in the SMC, we find that the mean size is $\sim$ 128 pc, the expansion velocity is 7.5 km s^{-1}, and the inferred kinematic age is 8 Myr. We also compute $E_{Hole} \sim 56 \times 10^{50}$, assuming an HI volume density of 1.0 cm^{-3}, and find that SFR$_{KA}$ = 7×10^{-5} M$_\odot$ yr^{-1}. We simulate 100 CMDs assuming a distance modulus of 19, photometric completeness limits of m$_V$ = 22 and m$_I$ = 21.7 (Harris & Zaritsky 2004), and the parameters listed in §3.2. We chose to only consider a burst model of SF at 8 Myr, since the differences between a burst and constant model of SF over such a short time scale are minimal. We ran 100 simulations, to account for small number statistics, and found that the typical CMD contained $\sim$ 40 stars (within the completeness limits) and the mean magnitude of the brightest star in the CMD was $\mathrm{m}_{F555W} \sim 14.80$. We found that only 25 out of the 100 simulated CMDs contained at least one star with $\mathrm{m}_{F555W} < 14$, i.e., a bright OB type star. For $\mathrm{m}_{F555W} < 15$, we found 72 CMDs contained at least one such star. This test signifies that for a episode of SF 8 Myr ago, only 25% of the time we would expect to find a star brighter than $\mathrm{m}_{F555W} = 14$, and 72% of the time for $\mathrm{m}_{F555W} = 15$.

Applying these statistics to the 509 holes cataloged by Hatzidimitriou et al. (2005), we expect 128 HI holes with at least one star brighter than $\mathrm{m}_{F555W} = 14$, or 367 holes for $\mathrm{m}_{F555W} = 15$. In comparison, Hatzidimitriou et al. (2005) find 330 HI holes with at least one star cluster, young star, or WR star. Initially, they also found 80 holes that appeared void of stars, however follow up observations revealed that 21 of the 80 holes appeared to have A spectral-type stars, leaving 59 holes without detected stellar companions, which is consistent with the 143 of holes we predict will appear void of MS stars at $\mathrm{m}_{F555W} = 15$. The uncertainties in our calculation are at least 50%, due to uncertainties in E_{Hole}, the stellar evolution models, and statistical error. Further, we are not able to test out results directly as we cannot reasonably compare our predicted stellar populations to the various catalogs used for correlations by Hatzidimitriou et al. (2005). However, we have demonstrated that even without the detection of a bright object inside a young HI hole, it is possible that the hole was created by stellar feedback.

6. Conclusions

In summary:

- The HST/ACS based CMDs of stars within HI holes from the catalogs of Puche et al. (1992) and Bagetakos et al. (2009) revealed significant stellar populations, including young MS and BHeBs with ages less than ~ 50 Myr, in *all* holes. We found that $\ll 1\%$ of the stars in the composite stellar population of either holes catalog were luminous MS stars less than ~ 10 Myr in age. This indicates that young OB associations are not reliable tracers of the locations of HI holes.

- We searched for differences in the stellar populations inside HI holes and those in selected control fields, regions similar in size to holes, but that span a wide range in HI column density. We found that, on average, the control fields have twice as many luminous (i.e., young) MS stars as the HI holes, however this is consistent with statistical fluctuations from small number statistics tests. We measured the SFHs and cumulative SFHs of both samples (holes and control fields) and found no significant differences. However, because we are not sensitive to holes less than ~ 100 pc in size, it could be that smaller holes are already forming in control fields. Only further similar studies involving an even wider range of hole sizes (e.g., SMC or LMC) can address this question with the requisite level of precision.

- Using the SFHs for stars in each hole as input into STARBURST99, we calculated the energy associated with SF over the past 200 Myr. From this we computed the energy input over the inferred kinematic age of each hole and calculated the feedback efficiency. Compared to theoretical values, 8 of the 23 P92 and 13 of the 19 THINGS holes have efficiencies greater 20%, with several exceeding 100%. Looking at the energy profiles over the last 200 Myr, we found that stellar feedback did produce enough energy, in principle, to have created all the HI holes, just not necessarily within the inferred kinematic age. This finding suggests that the inferred kinematic age (which is poorly constrained from observations) may not represent the true age of an individual HI hole. Indeed, the concept of an age for an HI hole created by multiple generations of SF is intrinsically ambiguous.

- Using the BHeBs from the full HST/ACS CMD of Ho II, we constructed two spatially resolved recent SFH movies of Ho II with look back times of ~ 100 Myr and ~ 200 Myr. Comparing these movies with the HI distribution, we found that low levels of SF have been common, and only in the past ~ 40 Myr has the SF rate elevated significantly. Since many of the holes are older than ~ 40 Myr, this suggests that holes are formed through a series of small SF events as opposed to a larger event at a single epoch.

- From the HST/ACS photometry, we constructed CMDs corresponding to the apertures used by Rhode et al. (1999). In all cases, we found mixed age stellar populations of hundreds or thousands of stars. Using Monte Carlo tests of synthetic CMDs and empirical comparisons from the HST/ACS photometry, we demonstrated that integrated light does not accurately trace the SFHs of stellar populations inside HI holes. We also show that young MS stars (< 75 Myr) are not highly clustered, which may imply that the single age stellar cluster method of HI formation is not the most likely model. This assumption can account for why Rhode et al. (1999) did not detect a greater number of holes with stars inside.

- Using the Monte Carlo technique, we computed expected stellar populations for HI holes outside the optical body of Ho II and found that low levels of SF ($\sim 10^{-5}$ M$_\odot$) could account for the presence of those holes. The remnant populations would be quite faint as only a handful of young stars would remain to be seen at the present time. We also examine the use of other SF tracers, Hα, 24μm, and UV, and find that at such low SFRs, they do not reliably correlate with the stellar populations of HI holes.

- We applied similar analysis to the 59 young (~ 8 Myr) HI holes that appear empty in the SMC (Hatzidimitriou et al. 2005), finding SFR$_{KA}$ = 7×10^{-5} M$_\odot$ yr^{-1}. Using the integrated stellar mass, we assume a burst of SFH at 8 Myr, and construct 100 simulated CMDs. The resulting synthetic stellar populations show that only 25% of the CMDs have at least one MS stars brighter than m$_{F555W}$ = 14 and 72% have at least one MS star brighter than m$_{F555W}$ = 15. Applying this to the 509 holes in the sample, we expect 128 HI holes with at least one bright star in the 25% case, 367 holes in the 72% case, and 143 holes to be without any MS star brighter than $m_{F555W} = 15$. Hatzidimitriou et al. (2005) find 330 holes that have at least one bright object, and 59 HI holes that do not have any objects. While this comparison is subject to large uncertainties, it demonstrates the plausibility of a stellar feedback origin for young HI holes without a bright stellar companion.

The evidence presented by the HST/ACS observations of Ho II suggests that stellar feedback provides enough energy, in principle, to create the observed HI holes in Ho II. The traditional theory that single epoch episodes of SF, and singled aged clusters, are responsible for HI hole creation is unlikely, because of the presence of mixed age stellar populations inside all of the holes, including holes with younger inferred ages. The conclusions of Rhode et al. (1999) and those in this paper are not contradicting, rather they both seem to reinforce the idea that HI holes are not often created by single aged stellar populations. The summation of the evidence is that the likely mechanism for the creation of HI holes is stellar feedback from SNe due to multiple generations of SF. An important caveat is found in the similarity of the stellar populations in control fields and the HI holes. While this detracts from the potential casual relationship between stellar feedback and HI hole creation, this result could simply be explained by the fact that we are not sensitive to holes smaller than $\sim$ 100 pc. Applying similar analysis to galaxies with a wider range in HI holes sizes (e.g., SMC or LMC) could reveal the extent of this effect and provide further insight into the potential link between stellar feedback and the formation and growth of HI holes.

7. Acknowledgments

Support for this work was provided by NASA through grant GO-10605 from the Space Telescope Science Institute, which is operated by AURA, Inc., under NASA contract NAS5-26555. DRW is grateful for support from a Penrose Fellowship. EDS is grateful for partial support from the University of Minnesota. This research has made use of NASA's Astrophysics Data System Bibliographic Services and the NASA/IPAC Extragalactic Database (NED), which is operated by the Jet Propulsion Laboratory, California Institute of Technology, under contract with the National Aeronautics and Space Administration. Special thanks to Ioannis Bagetakos and Elias Brinks for sharing their data and results before publication and providing useful guidance. We would also like to thank Cliff Johnson and Danny Dale for making calibrated *Spitzer* image of Ho II available and Julianne Dalcanton for her insightful comments.

REFERENCES

Bagetakos, I., Brinks, E., Walter, F., de Blok, W. J. G., Rich, J. W., Usero, A., & Kennicutt, R. C., Jr. 2009, submitted.

Bastian, N., Gieles, M., Ercolano, B., & Gutermuth, R. 2009, MNRAS, 392, 868

Book, L. G., Chu, Y.-H., & Gruendl, R. A. 2008, ApJS, 175, 165

Brinks, E., & Bajaja, E. 1986, A&A, 169, 14

Brinks, E., & Burton, W. B. 1984, A&A, 141, 195

Bureau, M., & Carignan, C. 2002, AJ, 123, 1316

Bureau, M., Walter, F., van Gorkom, J., & Carignan, C. 2004, Recycling Intergalactic and Interstellar Matter, 217, 452

Calzetti, D., et al. 2007, ApJ, 666, 870

Cannon, J. M., et al. 2005, ApJ, 630, L37

Cash, W., Charles, P., Bowyer, S., Walter, F., Garmire, G., & Riegler, G. 1980, ApJ, 238, L71

Chandar, R., Leitherer, C., Tremonti, C. A., Calzetti, D., Aloisi, A., Meurer, G. R., & de Mello, D. 2005, ApJ, 628, 210

Chevalier, R. A. 1974, ApJ, 188, 501

Chu, Y.-H. 2008, IAU Symposium, 250, 341

Cole, S., Aragon-Salamanca, A., Frenk, C. S., Navarro, J. F., & Zepf, S. E. 1994, MNRAS, 271, 781

Dalcanton, J. J., et al. 2009, ApJS, 183, 67

Dale, D., et al. 2009, accepted to ApJ

Deul, E. R., & den Hartog, R. H. 1990, A&A, 229, 362

Dib, S., & Burkert, A. 2005, ApJ, 630, 238

Dohm-Palmer, R. C., et al. 1997, AJ, 114, 2527

Dohm-Palmer, R. C., & Skillman, E. D. 2002, AJ, 123, 1433

Dolphin, A. E. 2000, PASP, 112, 1383

Dolphin, A. E. 2002, MNRAS, 332, 91

Elmegreen, B. G. 1997, ApJ, 477, 196

Ford, H. C., et al. 1998, Proc. SPIE, 3356, 234

Gallart, C., Aparicio, A., Bertelli, G., & Chiosi, C. 1996, AJ, 112, 1950

Gallart, C., Zoccali, M., & Aparicio, A. 2005, ARA&A, 43, 387

Gieles, M., Bastian, N., & Ercolano, B. 2008, MNRAS, 391, L93

Gil de Paz, A., et al. 2007, ApJS, 173, 185

Harris, J., & Zaritsky, D. 2004, AJ, 127, 1531

Harris, J., & Zaritsky, D. 2008, Publications of the Astronomical Society of Australia, 25, 116

Hatzidimitriou, D., Stanimirovic, S., Maragoudaki, F., Staveley-Smith, L., Dapergolas, A., & Bratsolis, E. 2005, MNRAS, 360, 1171

Heiles, C. 1979, ApJ, 229, 533

Heiles, C. 1990, ApJ, 354, 483

Hernandez, X., Valls-Gabaud, D.,& Gilmore, G. 1999, MNRAS, 304, 705

Holtzman, J. A., et al. 1999, AJ, 118, 2262

Ikuta, C., & Arimoto, N. 2002, A&A, 391, 55

Jackson, D. C., Cannon, J. M., Skillman, E. D., Lee, H., Gehrz, R. D., Woodward, C. E., & Polomski, E. 2006, ApJ, 646, 192

Karachentsev, I. D., et al. 2002, A&A, 383, 125

Kennicutt, R. C., Jr. 1989, ApJ, 344, 685

Kennicutt, R. C., Jr. 1998, ARA&A, 36, 189

Kennicutt, R. C., Jr., et al. 2003, PASP, 115, 928

Kennicutt, R. C., Jr., et al. 2007, ApJ, 671, 333

Kennicutt, R. C., Jr., Lee, J. C., Funes, S. J., José G., Sakai, S., & Akiyama, S. 2008, ApJS, 178, 247

Kellman, S. A. 1970, Ph.D. Thesis

Kim, S., Dopita, M. A., Staveley-Smith, L., & Bessell, M. S. 1999, AJ, 118, 2797

Lada, C. J., & Lada, E. A. 2003, ARA&A, 41, 57

Lee, J. C., et al. 2008, Astronomical Society of the Pacific Conference Series, 396, 151

Leitherer, C., et al. 1999, ApJS, 123, 3

Loeb, A., & Perna, R. 1998, ApJ, 503, L35

Marigo, P., Girardi, L., Bressan, A., Groenewegen, M. A. T., Silva, L., & Granato, G. L. 2008, A&A, 482, 883

McCray, R., & Kafatos, M. 1987, ApJ, 317, 190

Meurer, G. R., et al. 2009, ApJ, 695, 765

Mighell, K. J. 1997, AJ, 114, 1458

Miller, B. W., & Hodge, P. 1996, ApJ, 458, 467

Muller, E., Staveley-Smith, L., Zealey, W., & Stanimirović, S. 2003, MNRAS, 339, 105

Oey, M. S., & Massey, P. 1995, ApJ, 452, 210

Oey, M. S., & Clarke, C. J. 1997, MNRAS, 289, 570

Oh, S.-H., de Blok, W. J. G., Walter, F., Brinks, E., & Kennicutt, R. C. 2008, AJ, 136, 2761

Padoan, P., Jimenez, R., & Jones, B. 1997, MNRAS, 285, 711

Pasquali, A., et al. 2008, ArXiv e-prints, 808, arXiv:0808.0193

Pflamm-Altenburg, J., Weidner, C., & Kroupa, P. 2007, ApJ, 671, 1550

Puche, D., Westpfahl, D., Brinks, E., & Roy, J.-R. 1992, AJ, 103, 1841

Recchi, S., & Hensler, G. 2006, A&A, 445, L39

Relaño, M., Beckman, J. E., Daigle, O., & Carignan, C. 2007, IAU Symposium, 237, 467

Rhode, K. L., Salzer, J. J., Westpfahl, D. J., & Radice, L. A. 1999, AJ, 118, 323

Sánchez-Salcedo, F. J. 2002, Revista Mexicana de Astronomia y Astrofisica, 38, 39

Scalo, J. M. 1986, Fundamentals of Cosmic Physics, 11, 1

Schlegel, D. J., Finkbeiner, D. P., & Davis, M. 1998, ApJ, 500, 525

Silich, S., Lozinskaya, T., Moiseev, A., Podorvanuk, N., Rosado, M., Borissova, J., & Valdez-Gutierrez, M. 2006, A&A, 448, 123

Skillman, E. D., Terlevich, R., Teuben, P. J., & van Woerden, H. 1988, A&A, 198, 33

Skillman, E. D. 1996, The Minnesota Lectures on Extragalactic Neutral Hydrogen, 106, 208

Stanimirović, S. 2007, IAU Symposium, 237, 84

Stewart, S. G., et al. 2000, ApJ, 529, 201 E., & de Blok, W. J. G. 2009, AJ, 137, 4424

Tenorio-Tagle, G., Bodenheimer, P., Rozyczka, M., & Franco, J. 1986, A&A, 170, 107

Tenorio-Tagle, G., & Bodenheimer, P. 1988, ARA&A, 26, 145

Theis, C., Burkert, A., & Hensler, G. 1992, A&A, 265, 465

Thilker, D. A., et al. 2007, ApJS, 173, 572

Thornton, K., Gaudlitz, M., Janka, H.-T., & Steinmetz, M. 1998, ApJ, 500, 95

Tolstoy, E., & Saha, A. 1996, ApJ, 462, 672

Tosi, M., Greggio, L., & Focardi, P. 1989, Ap&SS, 156, 295

Tremonti, C. A., Calzetti, D., Leitherer, C., & Heckman, T. M. 2001, ApJ, 555, 322

Tremonti, C. A., Lee, J. C., van Zee, L., Kennicutt, R. C., Gil de Paz, A., Sakai, S., Funes, J., & Akiyama, S. 2007, Bulletin of the American Astronomical Society, 38, 894

van der Hulst, J. M. 1996, The Minnesota Lectures on Extragalactic Neutral Hydrogen, 106, 47

Walter, F., & Brinks, E. 1999, AJ, 118, 273

Walter, F., Brinks, E., de Blok, W. J. G., Bigiel, F., Kennicutt, R. C., Thornley, M. D., & Leroy, A. 2008, AJ, 136, 2563

Weaver, R., McCray, R., Castor, J., Shapiro, P., & Moore, R. 1977, ApJ, 218, 377

Weidner, C., & Kroupa, P. 2006, MNRAS, 365, 1333

Weisz, D. R., Skillman, E. D., Cannon, J. M., Dolphin, A. E., Kennicutt, R. C., Jr., Lee, J.C.,& Walter, F. 2008, ApJ, 689,160

Weisz, D. R., Skillman, E. D., Cannon, J. M., Walter, F., Brinks, E., Ott, J., & Dolphin, A. E. 2009, ApJ, 691, L59

Yuk, I.-S., & Lee, M. G. 2007, ApJ, 668, 876

This preprint was prepared with the AAS LaTeX macros v5.2.

Table 1. Photometric Properties of Puche et al. HI Holes

Hole Number (1)	α (J2000) (2)	δ (J2000) (3)	Diameter (arcsec) (4)	No. of Stars in CMD (5)	Integrated m_{F555W} (6)
10	8 18 42	+70 41 21	73	4149	17.68
12	8 13 49	+70 43 33	22	2065	18.65
14	8 18 56	+70 43 27	27	3907	17.47
16	8 18 59	+70 43 51	13	948	19.00
20	8 19 01	+70 42 44	8	383	20.19
21	8 19 04	+70 41 16	115	39153	14.72
22	8 19 06	+70 43 08	32	6443	16.65
23	8 19 06	+70 43 30	39	9477	16.22
24	8 19 08	+70 44 03	10	579	19.37
28	8 19 13	+70 43 31	19	1934	17.93
29	8 19 14	+70 42 21	27	4517	17.58
30	8 19 14	+70 44 20	69	20614	15.77
31	8 19 15	+70 43 49	18	1625	18.37
32	8 19 16	+70 41 49	37	3782	17.83
33	8 19 17	+70 44 56	25	2140	18.34
36	8 19 19	+70 43 14	37	5945	16.98
37	8 19 20	+70 45 17	20	1011	19.12
39	8 19 23	+70 44 43	23	1971	18.24
42	8 19 25	+70 45 12	22	1383	18.75
43	8 19 27	+70 42 06	16	549	18.75
44	8 19 27	+70 43 31	48	7566	16.82
45	8 19 27	+70 45 19	32	2344	18.08
48	8 19 36	+70 44 54	50	4695	16.93

Note. — Numbers, coordinates, and diameters for each hole taken from Puche et al. (1992). Hole coordinates have been converted to the J2000 epoch for ease of comparison.

Table 2. Photometric Properties of THINGS HI Holes

Hole Number (1)	α (J2000) (2)	δ (J2000) (3)	Diameter (arcsec) (4)	No. of Stars in CMD (5)	Integrated m_{F555W} (6)
4	8 18 40	+70 41 36	44	1733	18.81
6	8 18 49	+70 43 40	29	3781	17.98
8	8 18 52	+70 42 46	21	2636	17.26
9	8 18 53	+70 44 27	17	1067	19.35
12	8 18 58	+70 42 56	24	4067	16.75
14	8 19 00	+70 42 26	19	2289	18.13
16	8 19 04	+70 43 28	46	16146	15.67
17	8 19 05	+70 41 24	128	61244	14.37
19	8 19 13	+70 44 24	67	25053	15.66
20	8 19 15	+70 45 25	20	1644	18.44
21	8 19 15	+70 45 01	23	2312	18.40
23	8 19 18	+70 43 21	45	11644	16.24
26	8 19 24	+70 43 29	29	4253	17.54
27	8 19 26	+70 42 14	19	1126	18.89
29	8 19 27	+70 45 29	29	2202	18.28
30	8 19 28	+70 44 38	19	1590	18.62
31	8 19 29	+70 43 38	30	3190	18.05
34	8 19 35	+70 45 05	40	3673	17.33
39	8 19 44	+70 43 55	29	640	19.31

Note. — HI holes from THINGS (Walter et al. 2008) that are within the HST/ACS field of view. Numbers, coordinates, and diameters for each HI hole are from Bagetakos et al. (2009)

Table 3. Derived Properties of Puche et al. HI Holes

Hole Number (1)	Diameter (pc) (2)	DV km s^{-1} (3)	Kinematic Age (Myr) (4)	E_{Hole} (P92) (10^{50} erg) (5)	E_{Hole} (new) (10^{50} erg) (6)	E_{SFKA} (10^{50} erg) (7)	Putative Efficiency_{KA} (8)
10	1171	8.8	65	500	364	2400	15%
12	349	7.7	22	18.0	16	130	12%
14	421	3.9	53	15.0	19	2700	0.7%
16	199	1.0	97	0.30	0.5	1000	<0.1%
20	125	6.5?	9.4	0.4	2.0	10	20%
21	1820	6.6	135	2800	7700	60000	13%
22	508	6.5	38	48.0	230	1600	15%
23	619	4.5	67	60	211	3300	6.4%
24	162	7.5?	11	1.66	5.0	20	27%
28	302	7.2?	21	11.0	83	220	37%
29	469	3.9	59	21.4	190	1300	15%
30	1083	8.1	65	737	2200	5700	39%
31	289	2.5?	56	2.20	13	900	1.4%
32	583	4.8	59	48.4	420	2600	16%
33	388	3.5	54	10.2	17	780	2.2%
36	579	8.3	34	119	990	1800	55%
37	312	11.9	13	28.8	34	45	74%
39	359	3.5	50	8.00	16	1500	1.1%
42	355	10.1	17	34.0	39	75	52%
43	255	4.8	26	3.73	25	90	28%
44	752	7.9	47	217	1200	7300	17%
45	596	6.6	37	53.5	51	930	6%
48	786	14.1	27	649	560	450	120%

Note. — (1) Hole numbers from Puche et al. (1992); (2) Hole diameters calculated assuming a distance of 3.4 Mpc; (3) Expansion velocities from Puche et al. (1992); (4) Kinematic age assumes the diameter from column 2 and expansion velocity from column 3; (5) Energy from Puche et al. (1992) was adjusted for a distance of 3.39 Mpc; (6) E_{Hole} computed using Equation 1 and the diameters and expansion velocities in this table, along with the values of n_0 computed in §4.1; (7) Total energy over the inferred kinematic age of the HI hole computed using STARBURST99; (8) The ratio of E_{Hole} to $E_{kinematic}$.

Table 4. Derived Properties of THINGS HI Holes

Hole Number (1)	Diameter (pc) (2)	DV km s^{-1} (3)	Kinematic Age (Myr) (4)	E_{Hole} (P92) (10^{50} erg) (5)	E_{Hole} (new) (10^{50} erg) (6)	E_{SFKA} (10^{50} erg) (7)	Putative Efficiency_{KA} (8)	Type (9)
4	731	7	51	100	170	500	34%	1
6	486	7	34	50	180	600	31%	1
8	345	10	17	32	140	500	28%	3
9	279	10	14	13	54	15	360%	3
12	403	11	18	63	450	330	140%	3
14	318	15	10	40	310	20	1600%	2
16	761	7	53	200	2100	4600	45%	1
17	2110	7	147	3200	18000	100000	18%	1
19	1107	7	77	500	3200	9500	34%	1
20	329	12	13	25	56	100	56%	3
21	378	9	21	20	88	300	29%	3
23	738	16	23	630	2900	2400	120%	2
26	483	7	34	50	133	2200	6%	1
27	312	7	22	20	25	190	13%	1
29	479	7	33	32	43	900	5%	1
30	318	13	12	32	40	150	26%	2
31	491	7	34	50	83	1000	8%	1
34	657	7	46	80	79	730	11%	1
39	474	18	13	160	66	50	130%	2

Note. — (1) − (5) Hole number, size, expansion, velocity, and E_{Hole} from the catalog of Bagetakos et al. (2009); (6) Total energy over the inferred kinematic age of the HI hole computed using STARBURST99; hole 6 had no appreciable SF within its kinematic age; (6) E_{Hole} computed using Equation 1 and the diameters and expansion velocities in this table, along with the values of n_0 computed in §4.1; (7) Total energy over the inferred kinematic age of the HI hole computed using STARBURST99; (8) Feeback efficiency: The ratio of E_{Hole} to E_{SFKA}; (8) The ratio of SFR_{KA} to the SFR averaged over the past 500 Myr. (9) Hole type as classified by Bagetakos et al. (2009), where type 1 holes are blown out and type 2 or 3 holes are still appreciably expanding.

Table 5. Photometric Properties of Control Fields

Hole Number (1)	α (J2000) (2)	δ (J2000) (3)	Aperture Diameter (arcsec) (4)	No. of Stars in CMD (5)	Integrated m_{F555W} (6)
c1	8 19 46	+70 44 29	30	839	19.38
c2	8 19 39	+70 43 55	30	1309	19.20
c3	8 19 28	+70 44 09	30	4089	17.64
c4	8 19 35	+70 43 08	30	1549	18.78
c5	8 19 32	+70 42 40	30	1863	18.08
c6	8 19 21	+70 42 28	30	3598	17.96
c7	8 19 12	+70 42 55	30	5183	17.40
c8	8 18 51	+70 42 05	30	1988	18.72
c9	8 18 45	+70 42 39	30	2147	17.74

Note. — Control fields shown in cyan in Figure 2. Corresponding CMDs in Figure 6 and SFHs in Figure 12.

Table 6. Photometric Properties of HI Holes used by Rhode et al. (1999)

Hole Number (1)	α (J2000) (2)	δ (J2000) (3)	Aperture Diameter (arcsec) (4)	No. of Stars in CMD (5)	Hole Type (6)	Integrated m_{F555W} (7)
10	8 18 40	+70 41 39	30.00	893	a	19.75
12	8 18 50	+70 43 41	20.00	1989	b	18.63
14	8 18 55	+70 43 34	20.00	2810	c	18.12
16	8 18 58	+70 43 01	20.00	2740	d	17.12
20	8 18 59	+70 42 52	20.00	2639	c	17.44
21	8 19 02	+70 41 21	30.00	4077	d	17.18
22	8 19 04	+70 43 16	20.00	3064	d	17.24
23	8 19 04	+70 43 40	20.00	3051	c	17.85
24	8 18 07	+70 44 14	20.00	2825	c	18.08
28	8 19 12	+70 43 52	20.00	2526	c	18.01
30	8 19 13	+70 44 32	20.00	2062	c	18.59
31	8 19 14	+70 44 04	20.00	2374	c	18.09
32	8 19 12	+70 41 54	24.00	2615	c	18.31
33	8 19 16	+70 45 10	20.00	1628	c	18.81
36	8 19 19	+70 43 21	24.00	3324	d	17.65
37	8 19 19	+70 45 32	20.00	1205	b	19.04
39	8 19 22	+70 44 51	20.00	1893	c	18.29
42	8 19 21	+70 45 21	20.00	1336	b	18.76
43	8 19 26	+70 42 16	16.00	805	e	19.40
44	8 19 24	+70 43 33	30.00	4229	d	17.60
45	8 19 25	+70 45 37	20.00	1023	c	19.04
48	8 19 35	+70 45 06	30.00	1892	d	18.14

Note. — (1) – (4) Numbers, coordinates, and diameters for each aperture taken from Rhode et al. (1999), which are based on the HI hole catalog of Puche et al. (1992). Coordinates have been converted to J2000 for ease of comparison; (6) Classifications from Rhode et al. (1999): a – empty hole, b – faint foreground star, c – galaxian background, d – possible star cluster, e – possible photoionization region; (7) integrated magnitudes calculated from the ACS CMDs (Figures 25 & 26).

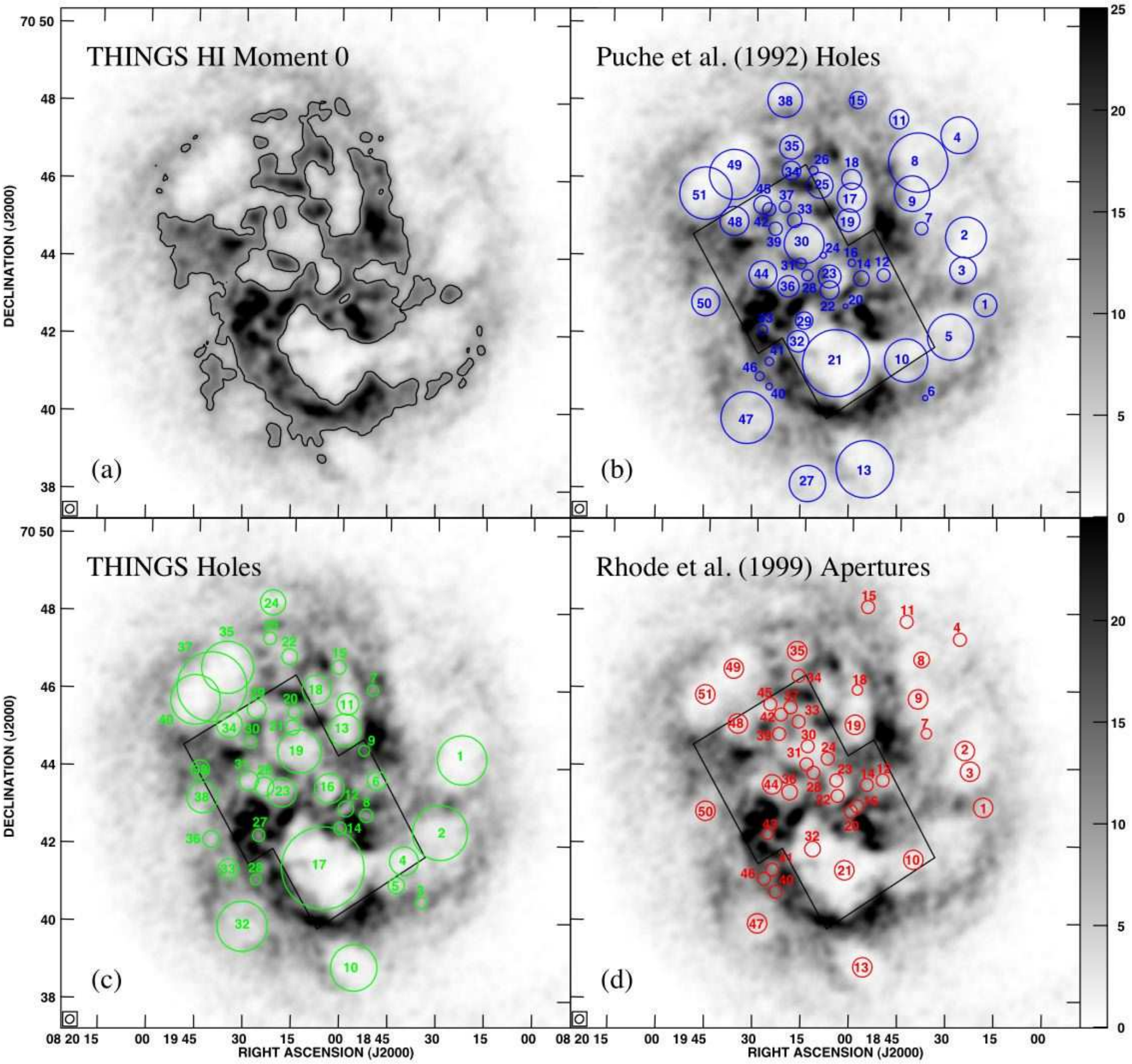

Fig. 1.— (a) HI surface density image of Ho II processed by the THINGS program (THINGS; Walter et al. 2008) with a contour of 10^{-21} cm^{-2} overlaid; (b) HI holes catalogued by Puche et al. (1992); (c) HI holes from the THINGS catalog (Bagetakos et al. 2009); (d) apertures used by Rhode et al. (1999) with the ACS footprint overlaid in black. Note the 'shredded' appearance of the HI distribution as well as the numerous separate holes cataloged in regions of low HI column density.

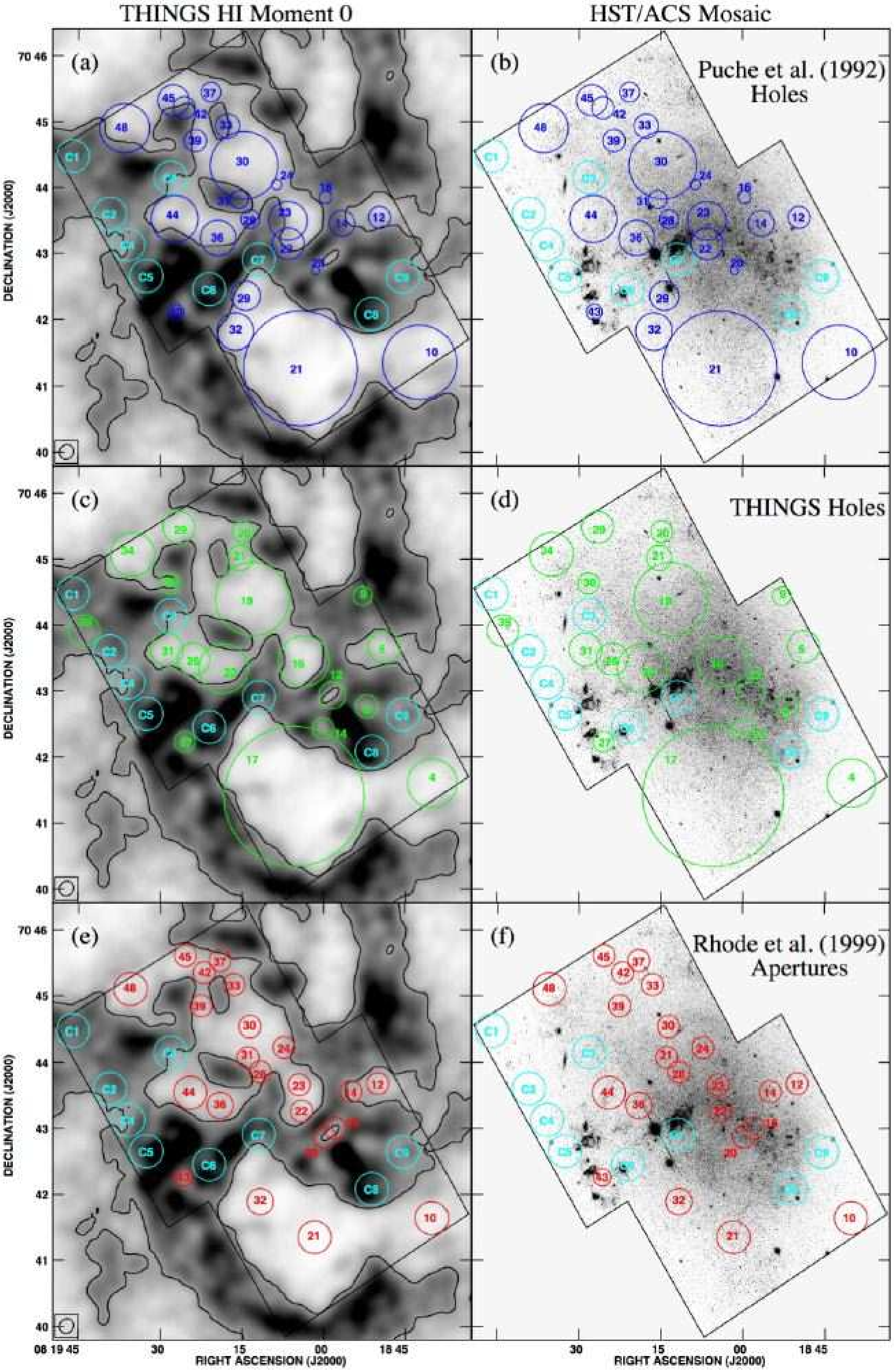

Fig. 2.— (a) THINGS processed HI image of Ho II (Walter et al. 2008) with a contour of 10^{-21} cm^{-2} overlaid and (b) ACS drizzled image of Ho II with Puche et al. (1992) holes in blue and control fields in cyan; (c) and (d) THING holes catalog (Bagetakos et al. 2009) in green and control fields in cyan; (e) and (f) Rhode et al. (1999) apertures in red and control fields in cyan.

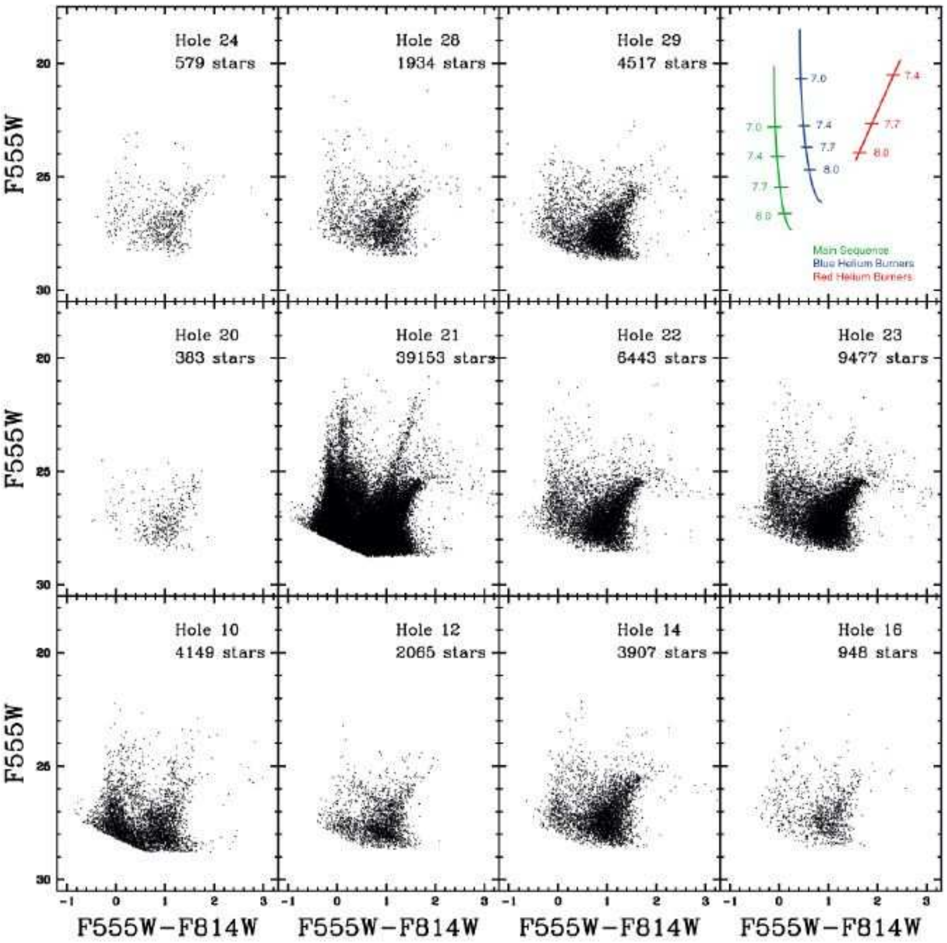

Fig. 3.— HST/ACS CMDs of the stars inside the HI holes cataloged by Puche et al. (1992), corrected for foreground reddening, $A_V = 0.11$ (Schlegel et al. 1998). The schematic in the upper right hand corner shows the ages of each type of star, MS (green), BHeB (green), and RHeB (red), with the logarithm of the ages (turn off age for the MS) shown as a function of magnitude and color on the CMD. Although sparse in some fields, note the presence of young MS and BHeB stars in all the CMDs. The fact the the BHeBs span a range in magnitudes indicate that multiple episodes of recent SF must have taken place, as different age BHeBs do not overlap on the CMD. In contrast, BHeBs from a single age cluster would have an overdensity at only one magnitude.

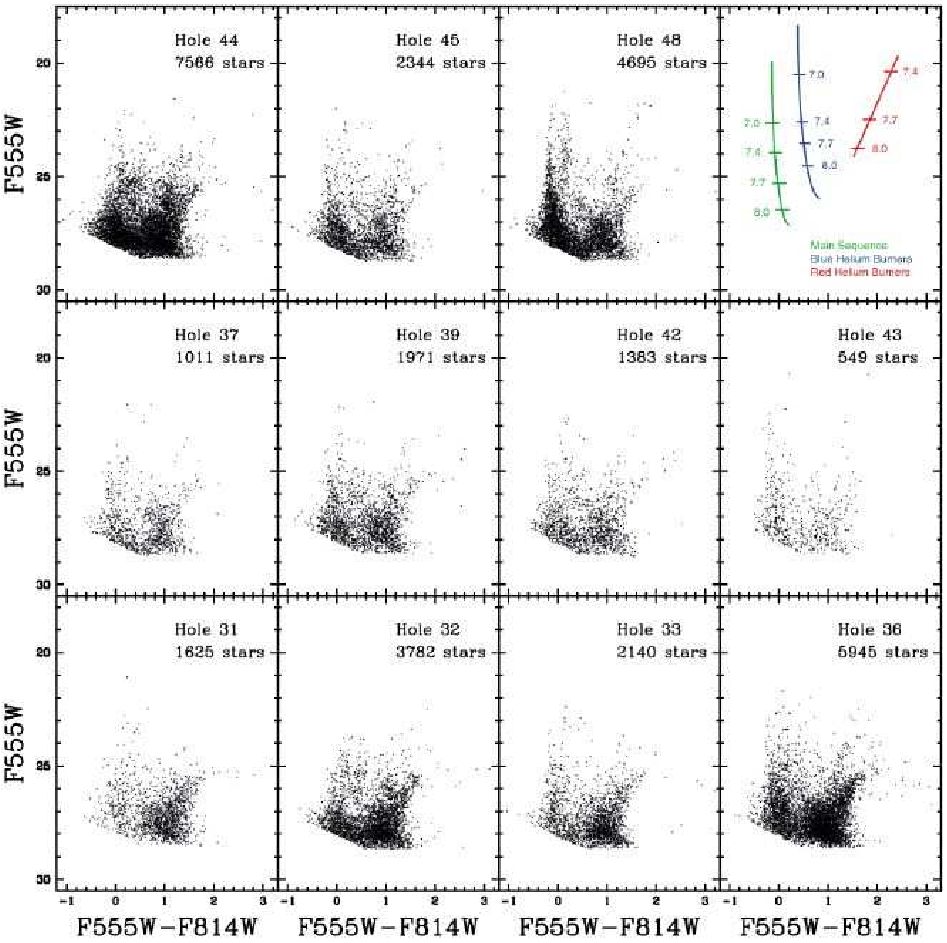

Fig. 4.— HST/ACS CMDs of the stars inside the HI holes cataloged by Puche et al. (1992), corrected for foreground reddening, $A_V = 0.11$ (Schlegel et al. 1998). The schematic in the upper right hand corner shows the ages of each type of star, MS (green), BHeB (green), and RHeB (red), with the logarithm of the ages (turn off age for the MS) shown as a function of magnitude and color on the CMD. Although sparse in some fields, note the presence of young MS and BHeB stars in all the CMDs. The fact the the BHeBs span a range in magnitudes indicate that multiple episodes of recent SF must have taken place, as different age BHeBs do not overlap on the CMD. In contrast, BHeBs from a single age cluster would have an overdensity at only one magnitude.

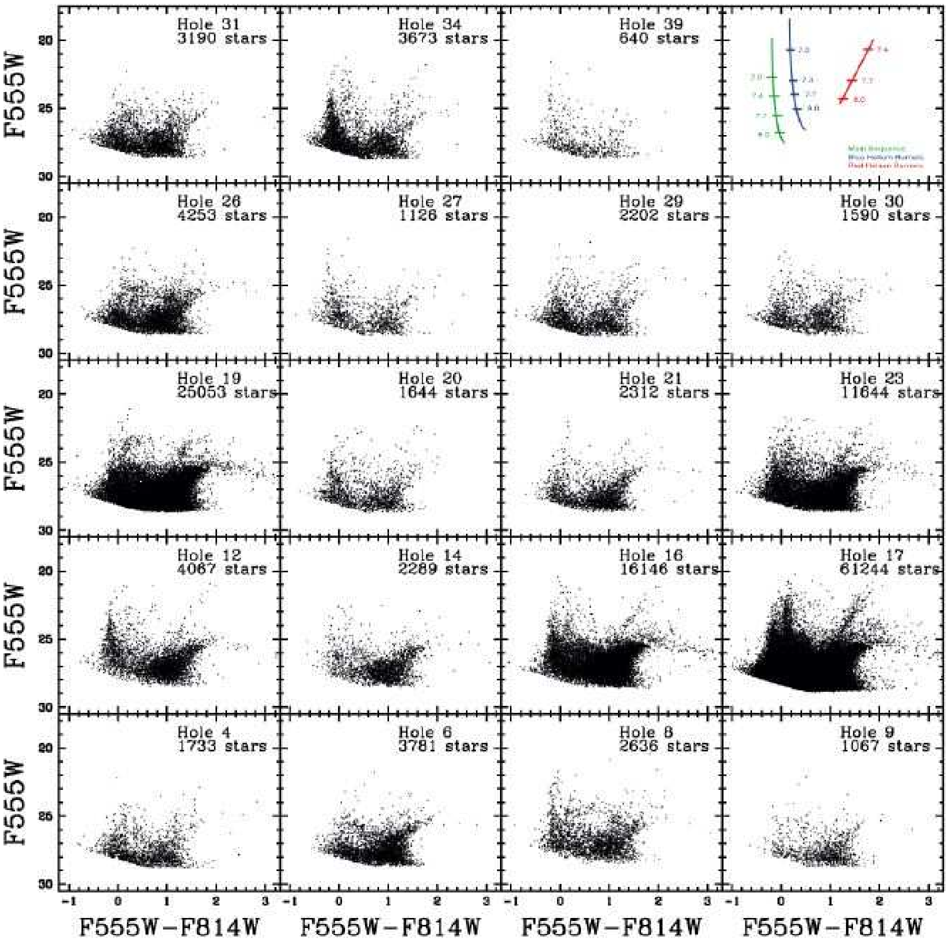

Fig. 5.— HST/ACS CMDs of the stars inside the HI holes cataloged by Bagetakos et al. (2009), corrected for foreground reddening, $A_V = 0.11$ (Schlegel et al. 1998). The schematic in the upper right hand corner shows the ages of each type of star, MS (green), BHeB (green), and RHeB (red), with the logarithm of the ages (turn off age for the MS) shown as a function of magnitude and color on the CMD. Although sparse in some fields, note the presence of young MS and BHeB stars in all the CMDs. The fact the the BHeBs span a range in magnitudes indicate that multiple episodes of recent SF must have taken place, as different age BHeBs do not overlap on the CMD. In contrast, BHeBs from a single age cluster would have an overdensity at only one magnitude.

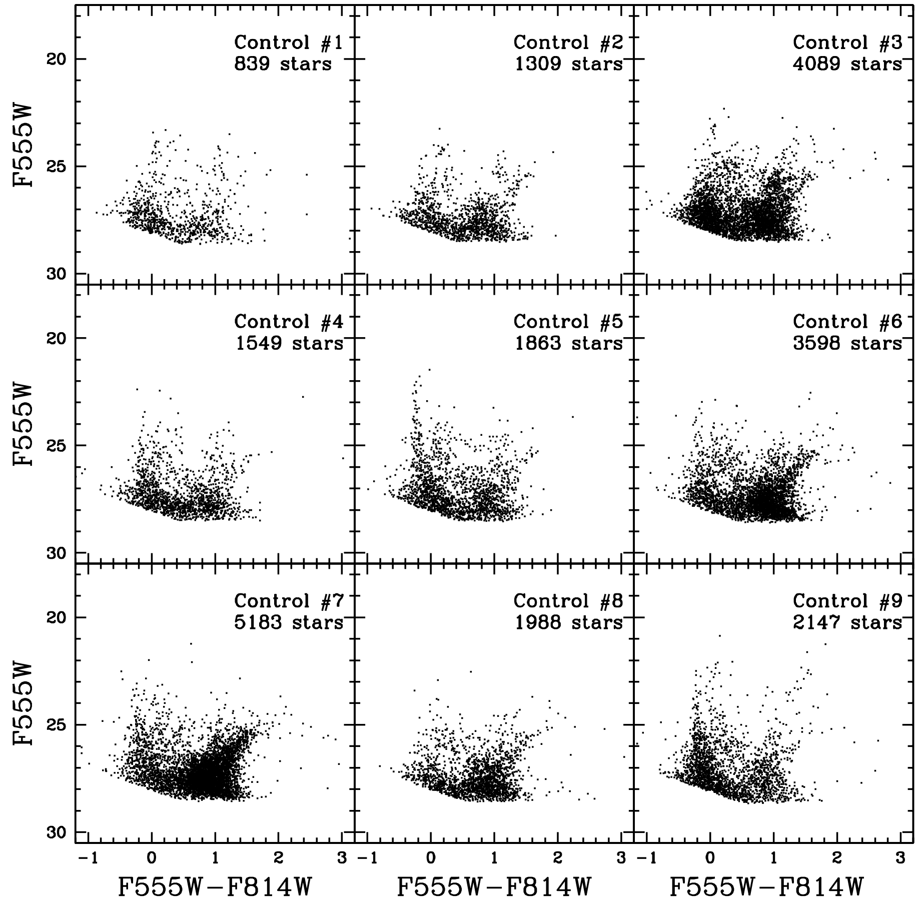

Fig. 6.— HST/ACS CMDs of the nine control fields in Ho II (Table 3 and Figure 2), corrected for foreground reddening, $A_V = 0.11$ (Schlegel et al. 1998). Although sparse in some fields, note the presence of young MS and BHeB stars in all the CMDs. The fact the the BHeBs span a range in magnitudes indicate that multiple episodes of recent SF must have taken place, as different age BHeBs do not overlap on the CMD. In contrast, BHeBs from a single age cluster would have an overdensity at only one magnitude. Comparing the CMDs of the control fields to those associated with the HI holes (Figure 3 − 5), there is not a clear difference in the composition of the two stellar populations despite having vastly different HI column densities.

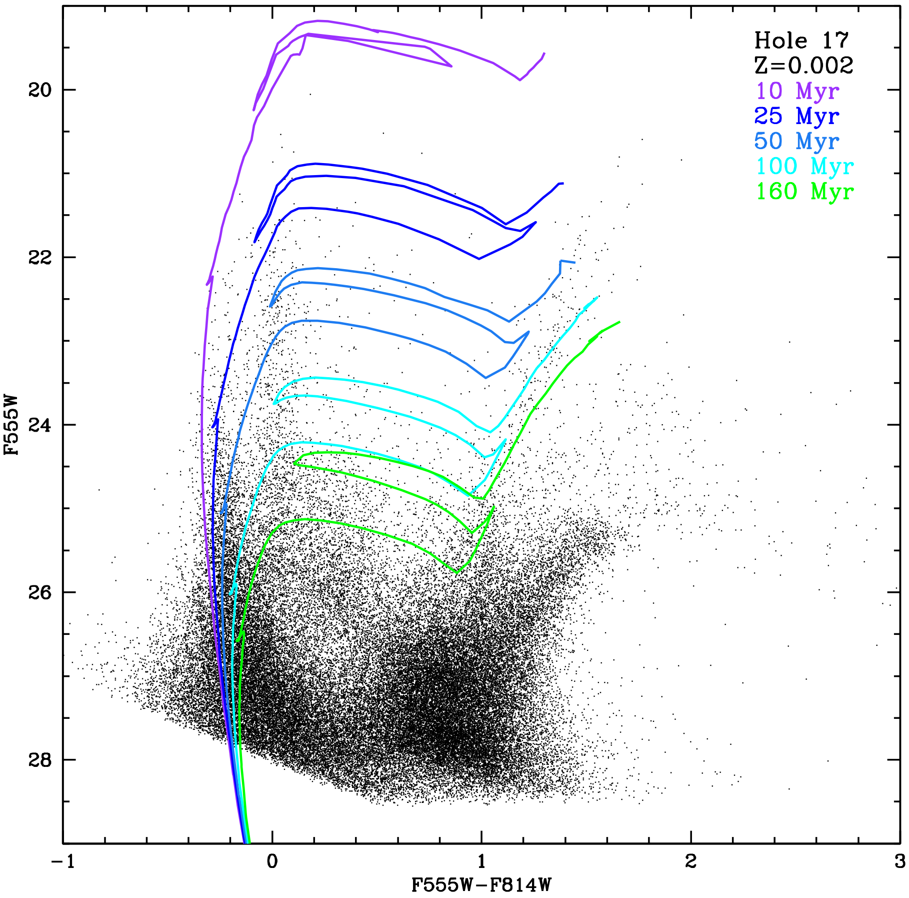

Fig. 7.— HST/ACS CMD of THINGS hole 17 with the Z=0.002 isochrones from Marigo et al. (2008) overlaid. The observed CMD has been corrected for foreground reddening. Notice that although the observed MS and isochrones show excellent agreement, the BHeB models become increasingly redder with age, when compared with the data. This is not an effect of metallicity, as we matched the isochrones to the measured nebular abundance (Miller & Hodge 1996). Instead, this is an example of the color mismatch for BHeB models at metallicites greater than $\sim 10\%$ $Z_{\odot}$.

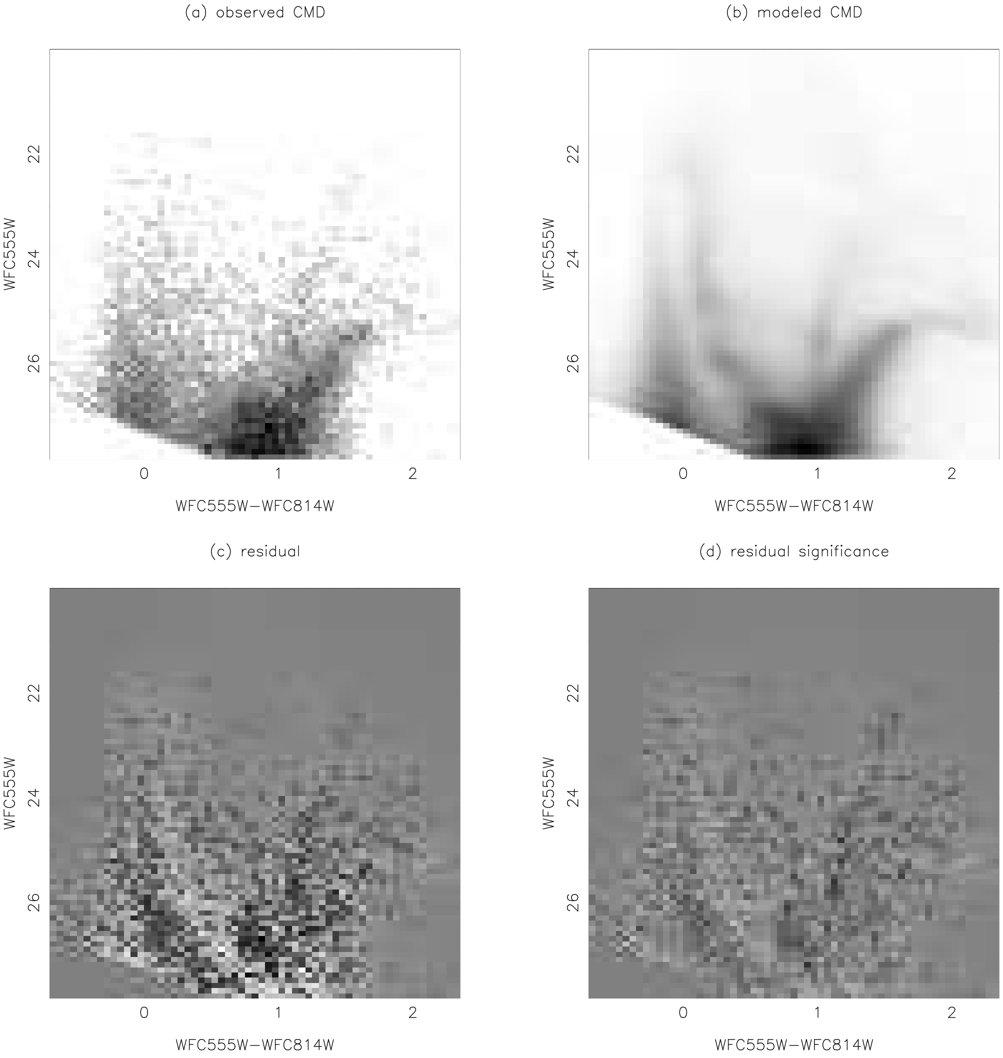

Fig. 8.— Comparison of the observed (panel (a)) and model CMDs (panel (b)) for THINGS hole 23 as measured using the code of Dolphin (2002). The bottom panels show the residual CMD (panel (c)) and the significance of the residuals (panel (d)). In the bottom panels black points indicate many more observed stars than synthetic star, while white points have more synthetic than observed stars. From the residual significance diagram we do not see any particularly poorly matched areas, indicating the synthetic CMD matches the data quite well.

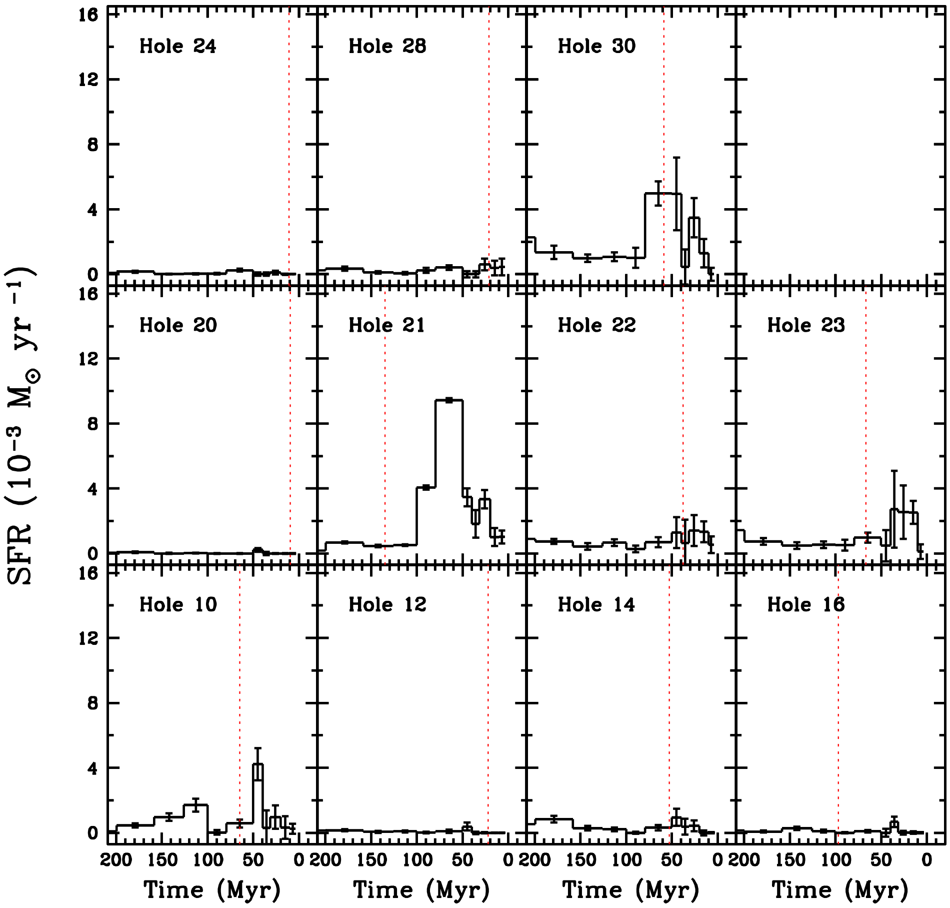

Fig. 9.— The recent SFHs of the stars inside the HI holes cataloged by Puche et al. (1992) over the last 200 Myr. The time resolution is ∼ 10 Myr until 50 Myr ago, and then ∼ 25 Myr there after. The red dotted line indicates the inferred kinematic age of each hole (Table 3). Note that the SFH of hole 21 has been scaled down by a factor of 10. In most cases, the majority of SF has taken place more recently than the inferred kinematic age, however, this is not always the case.

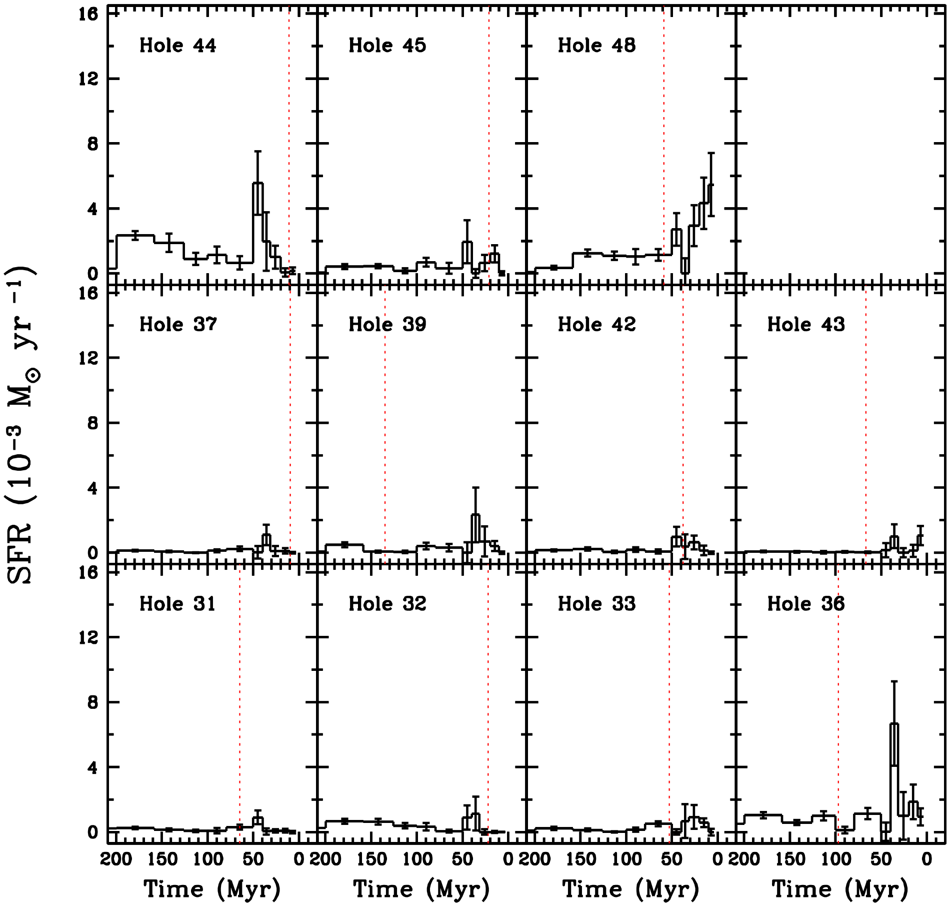

Fig. 10.— The recent SFHs of the stars inside the HI holes cataloged by Puche et al. (1992) over the last 200 Myr. The time resolution is ∼ 10 Myr until 50 Myr ago, and then ∼ 25 Myr there after. The red dotted line indicates the inferred kinematic age of each hole (Table 3). In most cases, the majority of SF has taken place more recently than the inferred kinematic age, however, this is not always the case.

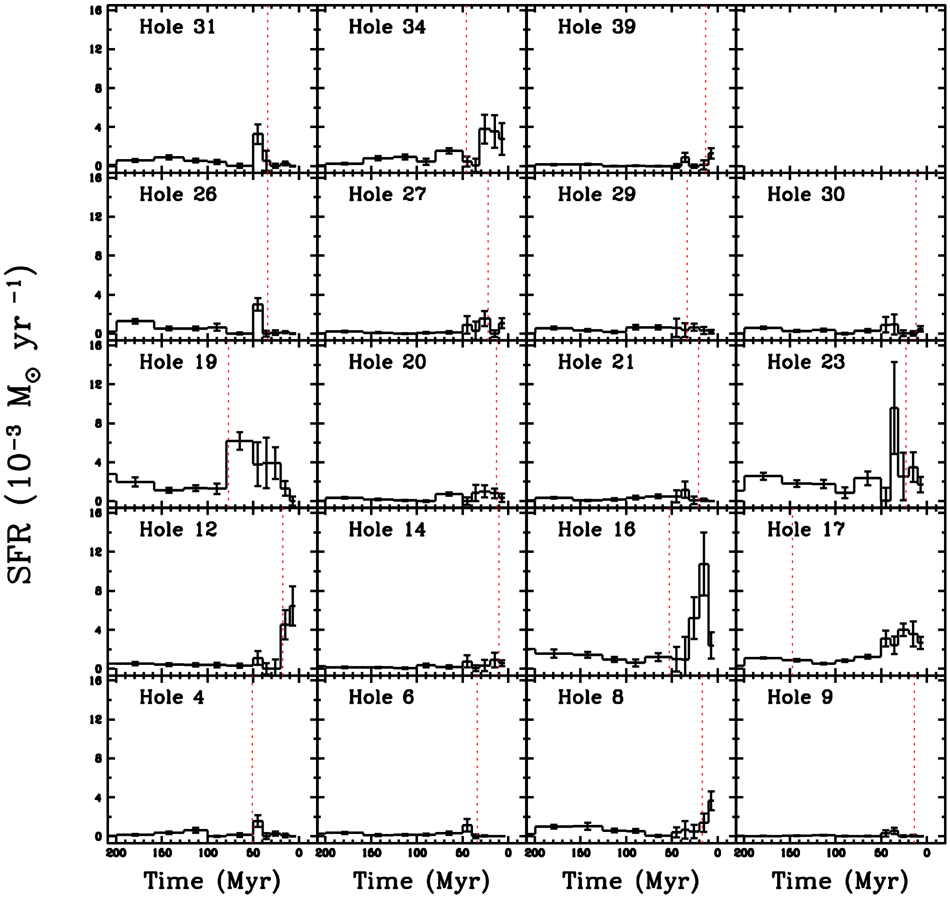

Fig. 11.— The recent SFHs of the stars inside the HI holes cataloged by Bagetakos et al. (2009) over the last 200 Myr. The time resolution is ∼ 10 Myr until 50 Myr ago, and then ∼ 25 Myr there after. The red dotted line indicates the kinematic age of each hole (Table 4). Note that the SFH of hole 17 has been scaled down by a factor of 10. In most cases, the majority of SF has taken place more recently than the inferred kinematic age, however, this is not always the case.

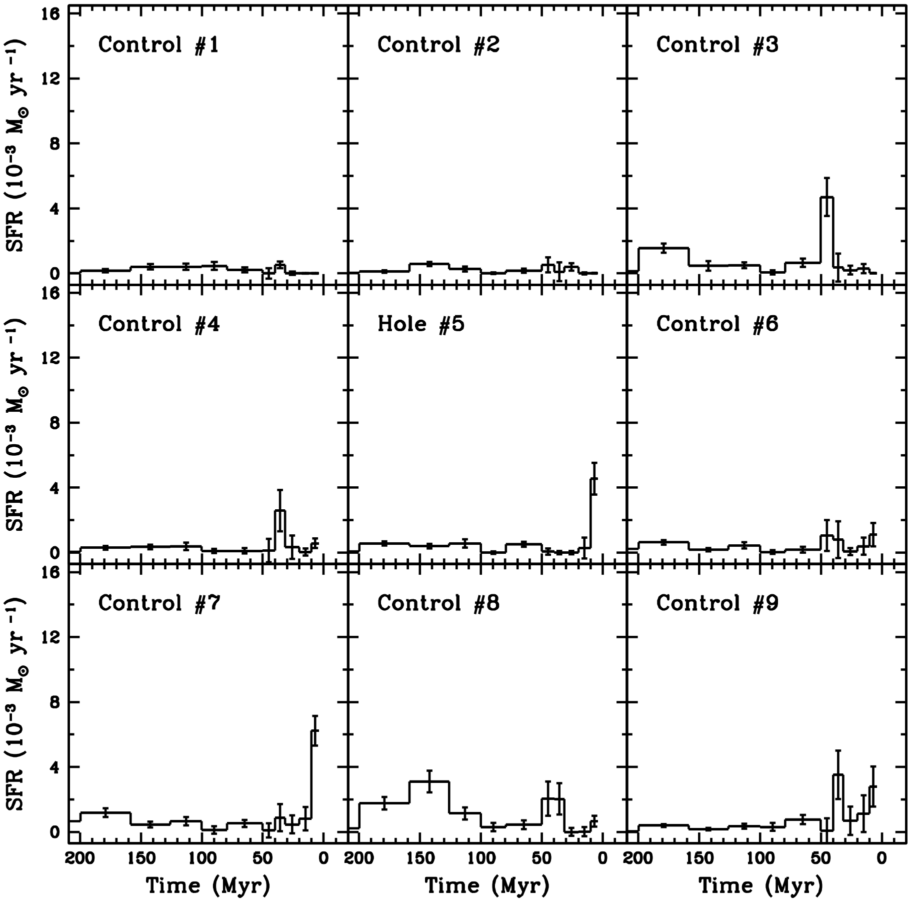

Fig. 12.— The recent SFHs of each control field in Ho II over the last 200 Myr. The time resolution is ∼10 Myr ber bin until 50 Myr and ∼ 25 Myr there after.

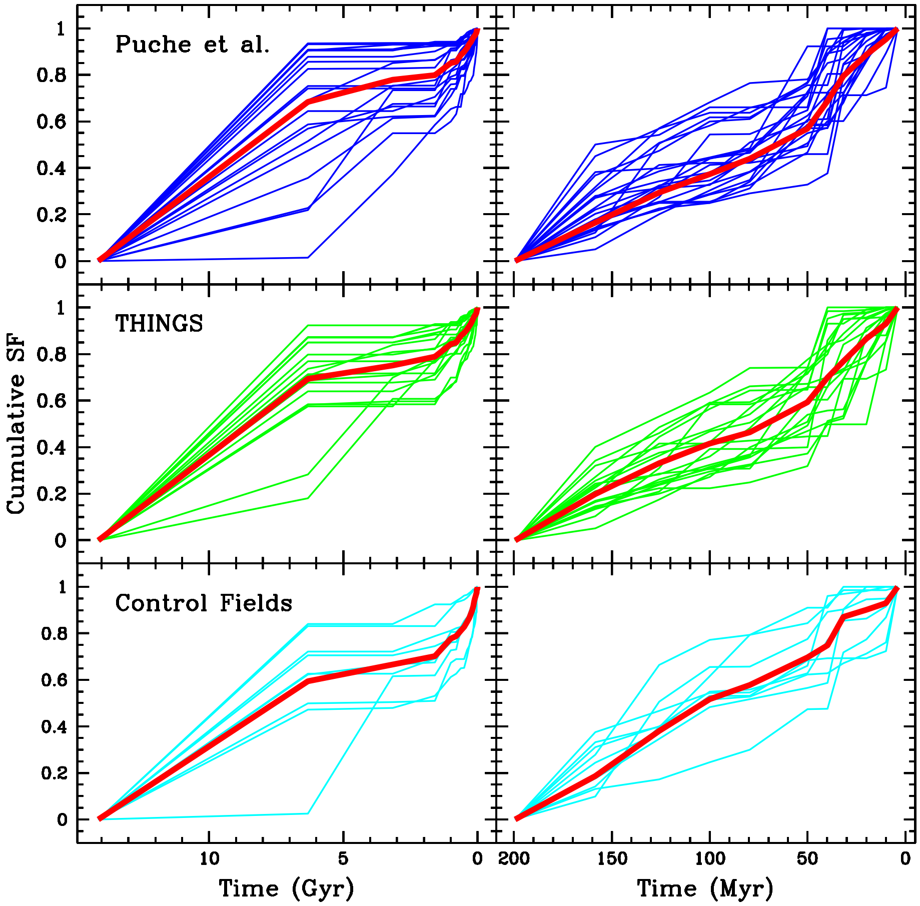

Fig. 13.— Comparison of the cumulative SF of stars within the holes from the Ho II for the Puche et al. (1992) catalog (blue) and the THINGS catalog (Bagetakos et al. 2009) (green) with the control fields cyan. The left panels show the cumulative SF over the the past 14.1 Gyr, while the panels on the right show the cumulative SF over the past 200 Myr. Although any given cumulative SFH is unique, a comparison of the HI holes and control fields suggest that the SFHs of the stars inside HI holes and the control fields are indistinguishable. For reference, the globally averaged SFR for the galaxy is 3.6×10^{-2} $M_\odot$ yr^{-1}, and the full SFH of the entire galaxy was measured by Weisz et al. (2008).

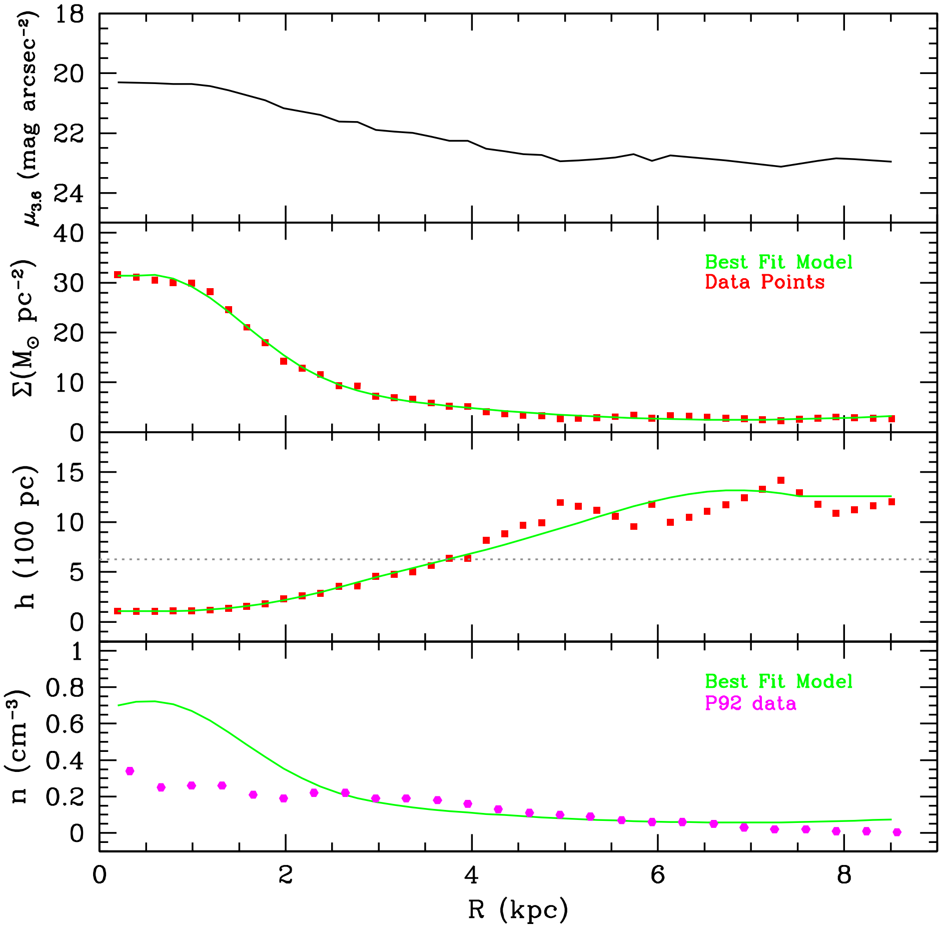

Fig. 14.— *Top panel*: Surface brightness profile of Ho II as measured from 3.6μm imaging from the Local Volume Legacy program (LVL; Lee et al. 2008; Dale et al. 2009) as a function of radius; *Second Panel*: The mass surface density derived from the surface brightness profile following the method of Oh et al. (2008). The red points are the data points and the green line is the best fit analytic function; *Third panel*: The gas scale height of Ho II as a function of radius assuming an isothermal disk derived using the method of (Kellman 1970; Kim et al. 1999). Data points are in red and the best fit analytic function is the green line. The grey dotted line is the constant value gas scale height used by (Puche et al. 1992); *Bottom Panel*: The present day HI volume density, n, as a function of radius (green line) with the values used by Puche et al. (1992) in magenta. Note the difference in the values of n between the best fit model obtained via surface photometry and the values used by Puche et al. (1992) in the inner $\sim$ 2 kpc. Because $E_{Hole} \propto n_0^{1.12}$ (where n_0 is the average volume density prior to hole formation), an increase in the volume density leads to an increase in the minimum energy necessary to create an HI hole. In this case n_0 measures the average value of the HI volume density, however, SF is more likely to occur at HI peaks, thus E_{Hole} is likely a lower bound (See §4.1 for more details).

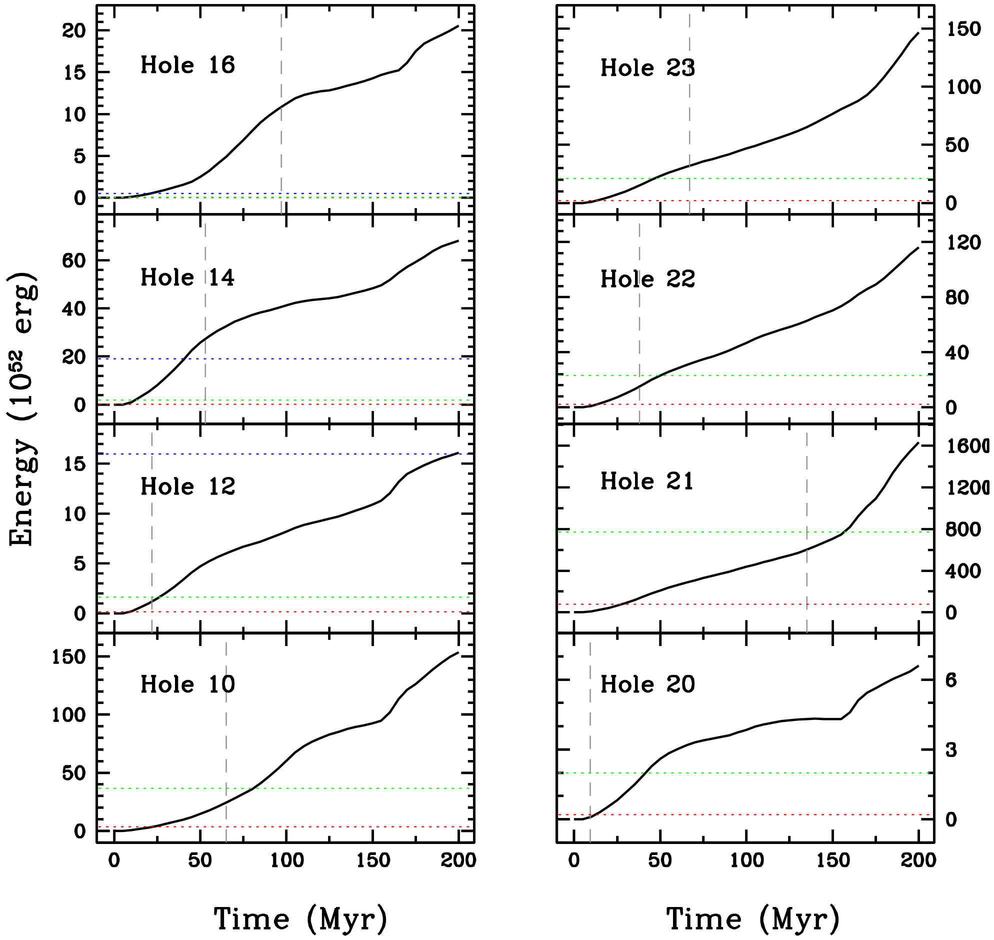

Fig. 15.— The cumulative energies of the stars inside the HI holes of Puche et al. (1992) computed using STARBURST99 (Leitherer et al. 1999) with the measured SFHs as input. The energies are integrated from the present (t = 0) over the past 200 Myr. The vertical grey dashed line is the kinematic age of each hole. The horizontal dotted lines are E_{Hole} assuming 100% (red), 10% (green), and 1% (blue) efficiencies. The intersection of the grey line with the energy profile indicates the putative feedback efficiency over the inferred kinematic age. In several cases, this falls outside the expected range, and may even be greater than 100%. This suggests that inferred kinematic age may not represent the true age of the hole. If instead, we use the intersection 10% efficiency line (green) and the energy profile as a guide, we can get a rough sense of how old the hole may be, if it formed from multiple generations of SNe.

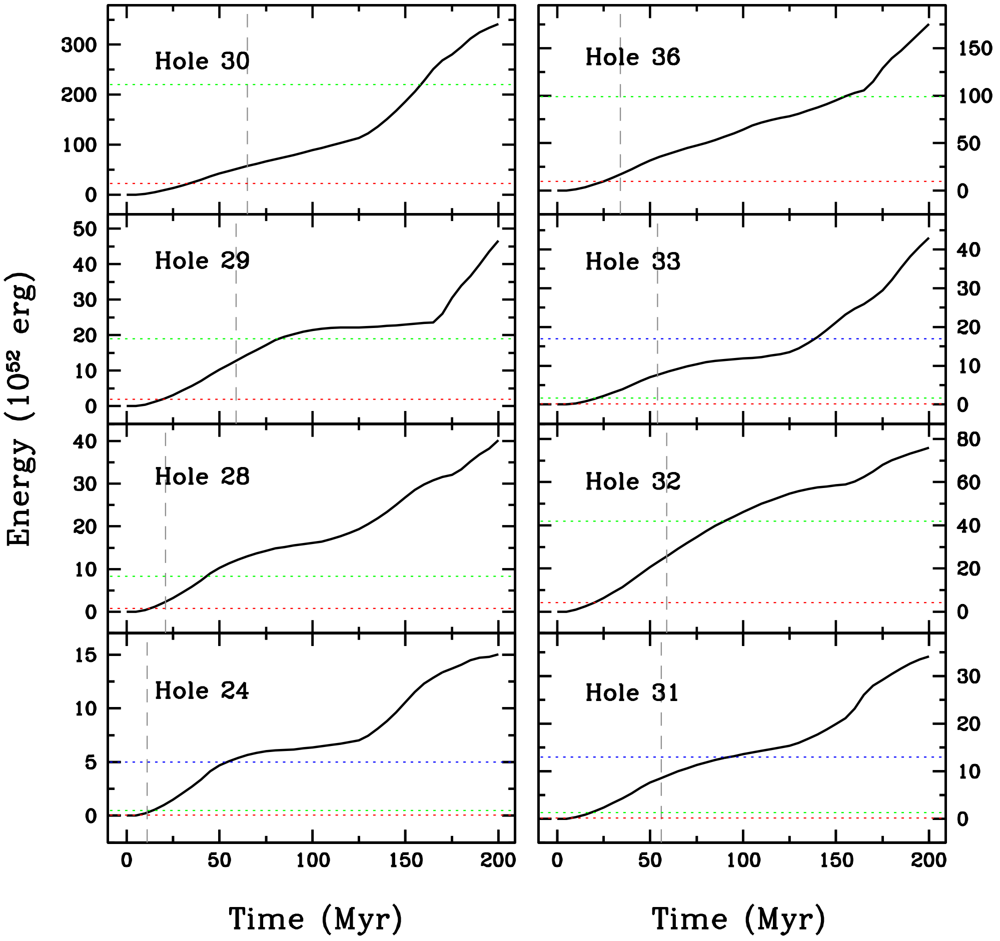

Fig. 16.— The cumulative energies of the stars inside the HI holes of Puche et al. (1992) computed using STARBURST99 (Leitherer et al. 1999) with the measured SFHs as input. The energies are integrated from the present (t = 0) over the past 200 Myr. The vertical grey dashed line is the kinematic age of each hole. The horizontal dotted lines are E_{Hole} assuming 100% (red), 10% (green), and 1% (blue) efficiencies. The intersection of the grey line with the energy profile indicates the putative feedback efficiency over the inferred kinematic age. In several cases, this falls outside the expected range, and may even be greater than 100%. This suggests that inferred kinematic age may not represent the true age of the hole. If instead, we use the intersection 10% efficiency line (green) and the energy profile as a guide, we can get a rough sense of how old the hole may be, if it formed from multiple generations of SNe.

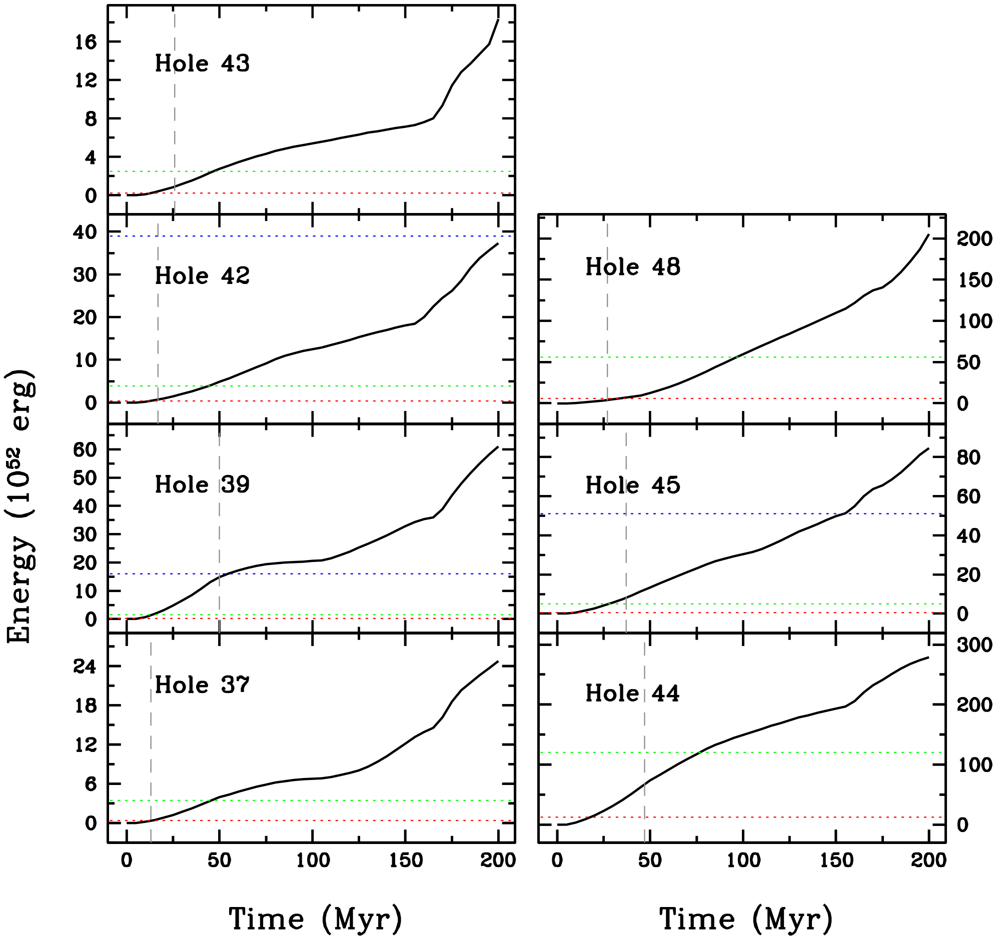

Fig. 17.— The cumulative energies of the stars inside the HI holes of Puche et al. (1992) computed using STARBURST99 (Leitherer et al. 1999) with the measured SFHs as input. The energies are integrated from the present (t = 0) over the past 200 Myr. The vertical grey dashed line is the kinematic age of each hole. The horizontal dotted lines are E_{Hole} assuming 100% (red), 10% (green), and 1% (blue) efficiencies. The intersection of the grey line with the energy profile indicates the putative feedback efficiency over the inferred kinematic age. In several cases, this falls outside the expected range, and may even be greater than 100%. This suggests that inferred kinematic age may not represent the true age of the hole. If instead, we use the intersection 10% efficiency line (green) and the energy profile as a guide, we can get a rough sense of how old the hole may be, if it formed from multiple generations of SNe.

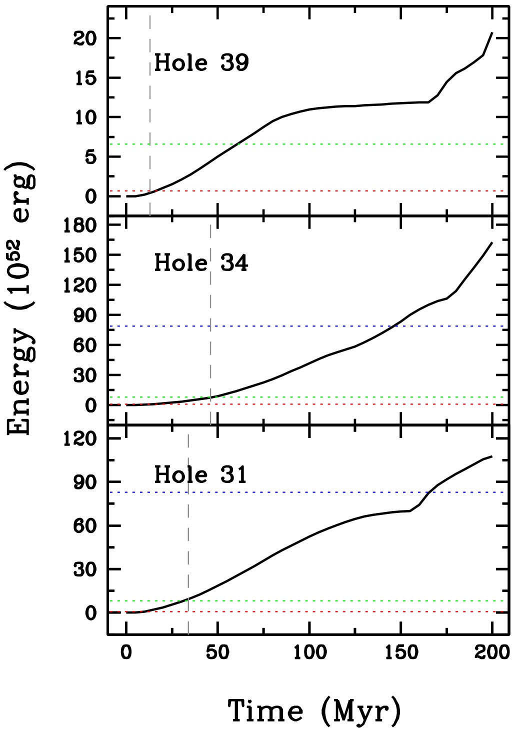

Fig. 18.— The cumulative energies of the stars inside the HI holes of Bagetakos et al. (2009) computed using STARBURST99 (Leitherer et al. 1999) with the measured SFHs as input. The energies are integrated from the present (t = 0) over the past 200 Myr. The vertical grey dashed line is the kinematic age of each hole. The horizontal dotted lines are E_{Hole} assuming 100% (red), 10% (green), and 1% (blue) efficiencies. The intersection of the grey line with the energy profile indicates the putative feedback efficiency over the inferred kinematic age. In several cases, this falls outside the expected range, and may even be greater than 100%. This suggests that inferred kinematic age may not represent the true age of the hole. If instead, we use the intersection 10% efficiency line (green) and the energy profile as a guide, we can get a rough sense of how old the hole may be, if it formed from multiple generations of SNe.

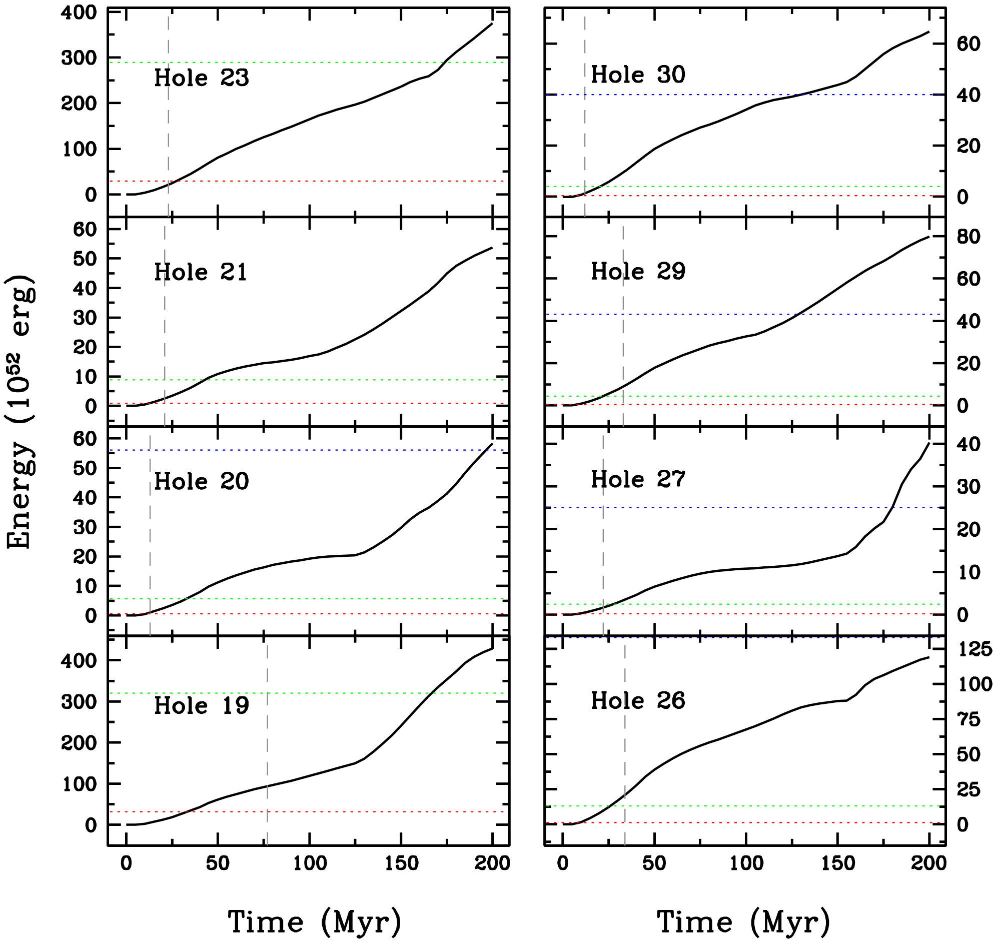

Fig. 19.— The cumulative energies of the stars inside the HI holes of Bagetakos et al. (2009) computed using STARBURST99 (Leitherer et al. 1999) with the measured SFHs as input. The energies are integrated from the present (t = 0) over the past 200 Myr. The vertical grey dashed line is the kinematic age of each hole. The horizontal dotted lines are E_{Hole} assuming 100% (red), 10% (green), and 1% (blue) efficiencies. The intersection of the grey line with the energy profile indicates the putative feedback efficiency over the inferred kinematic age. In several cases, this falls outside the expected range, and may even be greater than 100%. This suggests that inferred kinematic age may not represent the true age of the hole. If instead, we use the intersection 10% efficiency line (green) and the energy profile as a guide, we can get a rough sense of how old the hole may be, if it formed from multiple generations of SNe.

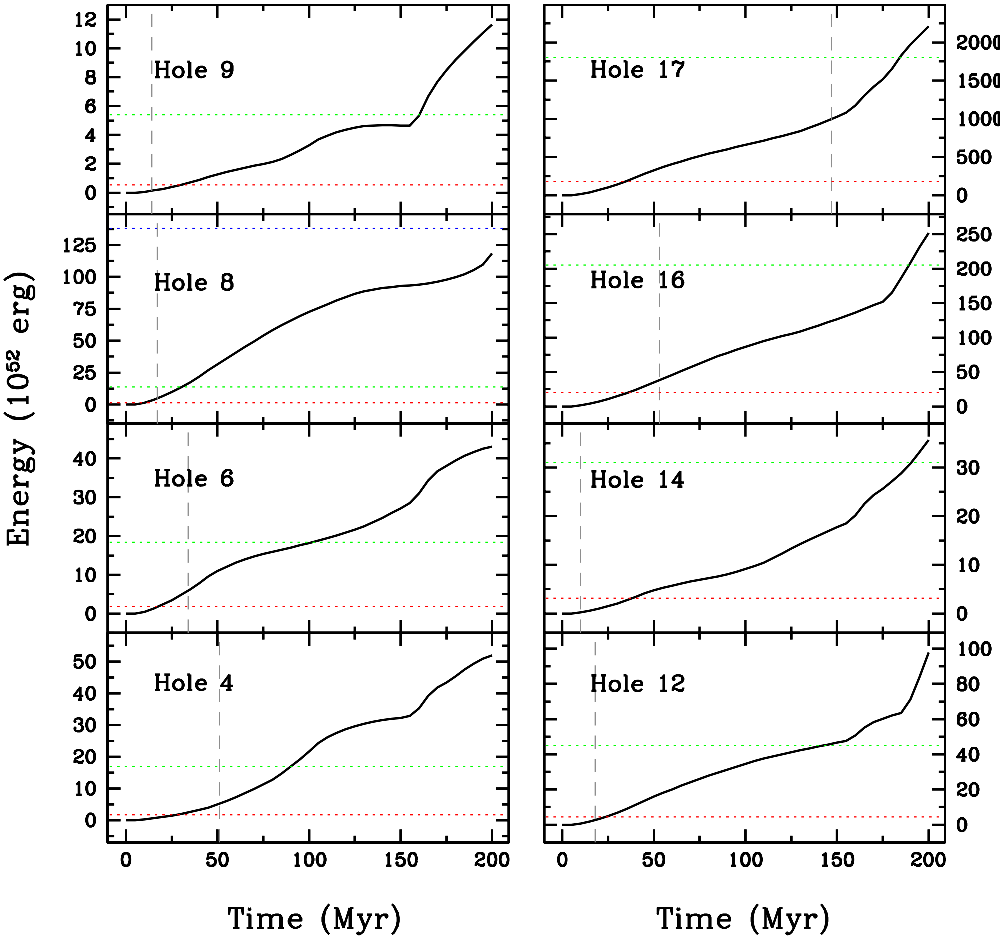

Fig. 20.— The cumulative energies of the stars inside the HI holes of Bagetakos et al. (2009) computed using STARBURST99 (Leitherer et al. 1999) with the measured SFHs as input. The energies are integrated from the present (t = 0) over the past 200 Myr. The vertical grey dashed line is the kinematic age of each hole. The horizontal dotted lines are E_{Hole} assuming 100% (red), 10% (green), and 1% (blue) efficiencies. The intersection of the grey line with the energy profile indicates the putative feedback efficiency over the inferred kinematic age. In several cases, this falls outside the expected range, and may even be greater than 100%. This suggests that inferred kinematic age may not represent the true age of the hole. If instead, we use the intersection 10% efficiency line (green) and the energy profile as a guide, we can get a rough sense of how old the hole may be, if it formed from multiple generations of SNe.

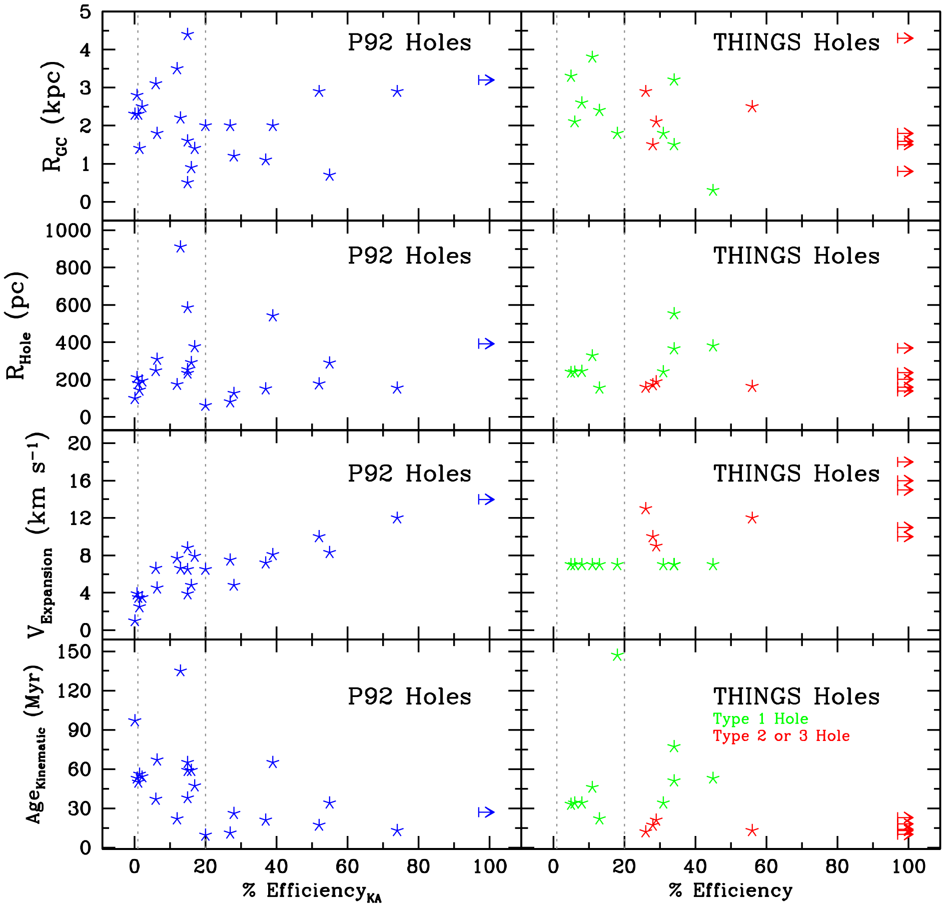

Fig. 21.— Putative stellar feedback efficiencies (E_{sfka}/E_{Hole}; Tables 3 and 4) plotted versus the galactrocentric radius (R_{GC}), hole radius (R_{Hole}), HI expansion velocity ($V_{Expansion}$), and kinematic age of each hole for the Puche et al. (1992) and the THINGS HI hole catalogs. For the THINGS holes, green stars are type 1 holes (blown out), the red stars are type 2 or 3 (not blown out), and the arrow indicate holes that have efficiencies greater than 100% and have been moved to fit the plot scale. The vertical grey dashed lines indicate the range of efficiencies predicted by various models, 1% – 20% (Theis et al. 1992; Cole et al. 1994; Padoan et al. 1997; Thornton et al. 1998). Note that the type 2 and 3 holes in the THINGS hole sample do not fall in to the expected range of putative feedback efficiency. These holes also tend to be young, expanding quickly, and are generally smaller in size. Arrows indicate lower limits on the efficiency for both hole catalogs.

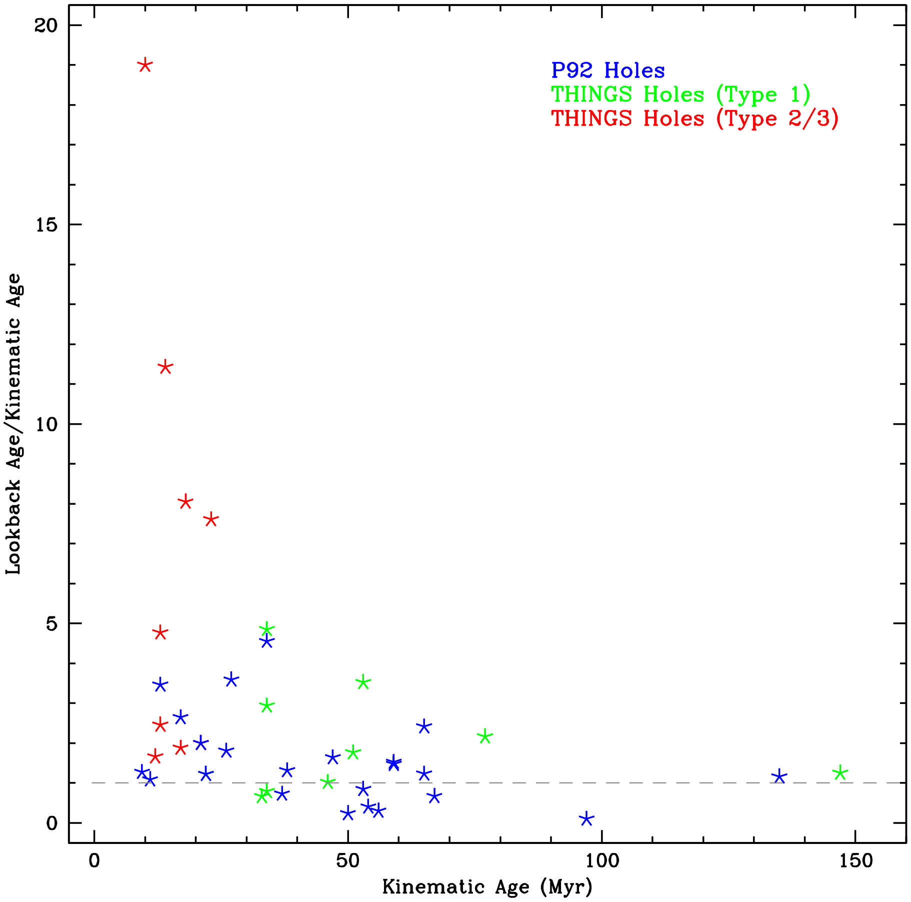

Fig. 22.— The ratio of look back age to inferred kinematic age for the HI holes from the Puche et al. (1992) and Bagetakos et al. (2009) as a function of the inferred kinematic age. The look back age is defined as the time at which the line of 10% efficiency intersects the energy profiles in Figures 15 − 20. The spread of values greater than unity (grey dashed line) implies that the inferred kinematic age often underestimates the age of HI holes, suggesting that the concept of an age for an HI hole created by multiple generations of SF is intrinsically ambiguous.

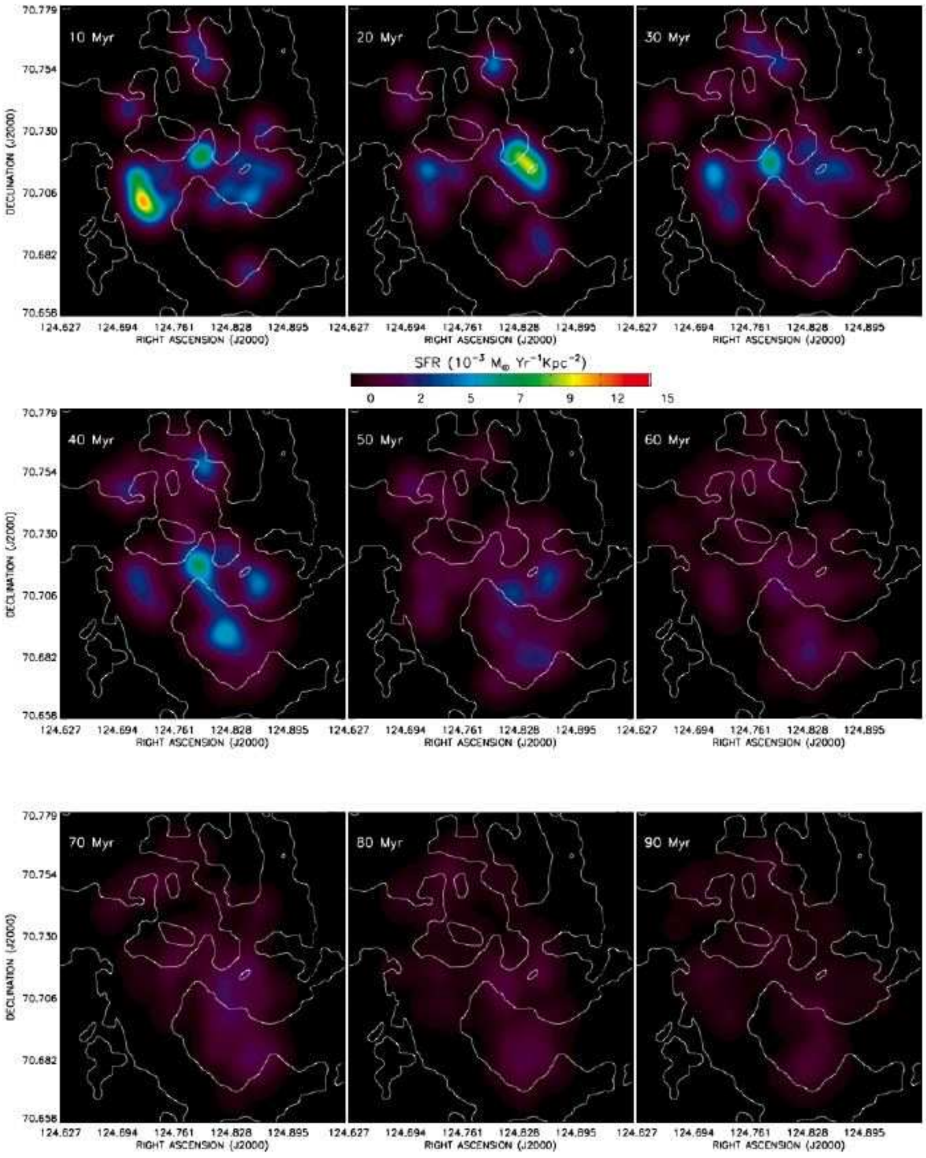

Fig. 23.— The spatially resolved recent SFH of Ho II over the last 90 Myr with 10 Myr time resolution as seen on the sky in units of SFR/area. The HI 10^{-21} cm^{-2} contour is overlaid in white. Note that majority of the galaxy is dominated by constant low level SF, while only a few regions have experienced elevated episodes of SF. As expected, the most recent frame shows the peaks of SF coincident with the peaks of the HI distribution.

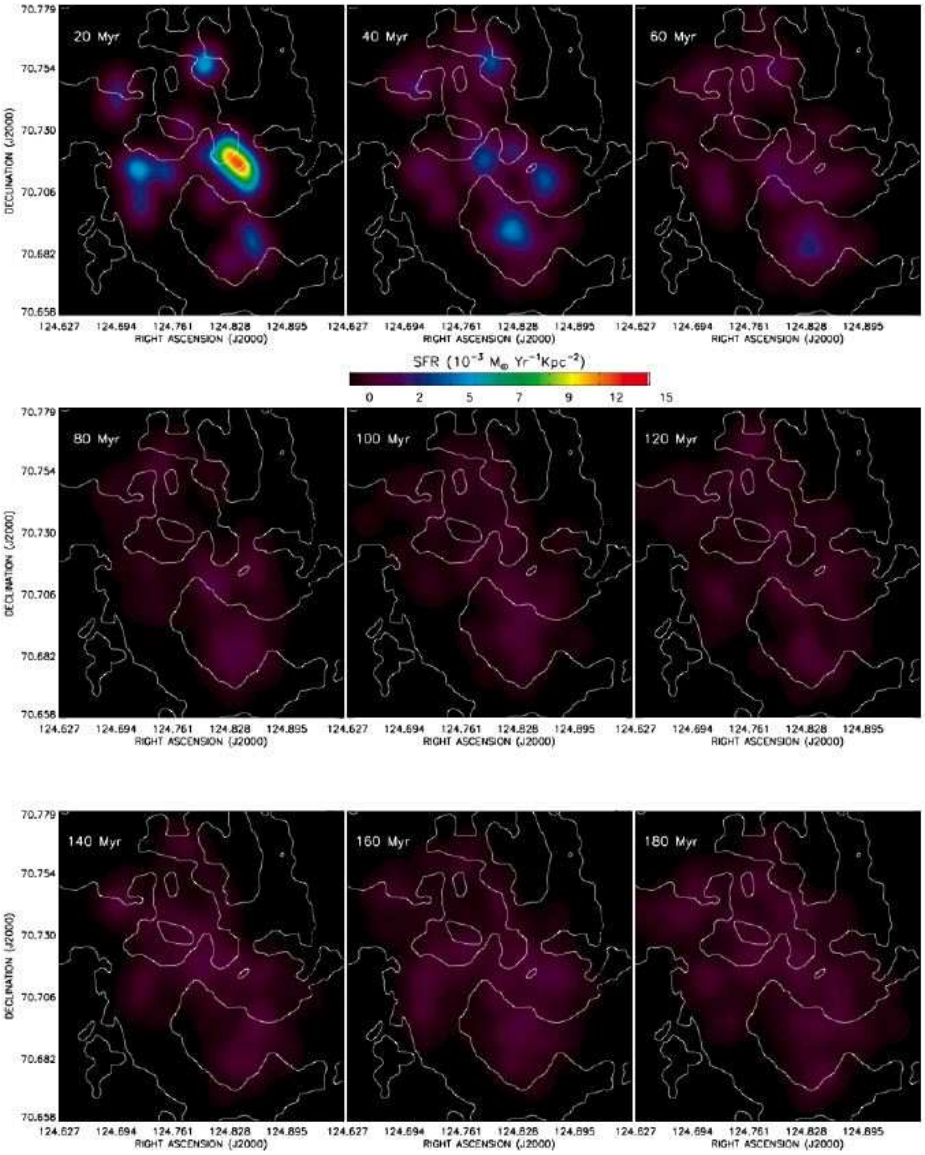

Fig. 24.— The spatially resolved recent SFH of Ho II over the last 180 Myr with 20 Myr time resolution as seen on the sky in units of SFR/area. The HI 10^{-21} cm^{-2} contour is overlaid in white. Note that majority of the galaxy is dominated by constant low level SF, while only a few regions have experienced elevated episodes of SF. As expected, the most recent frame shows the peaks of SF coincident with the peaks of the HI distribution.

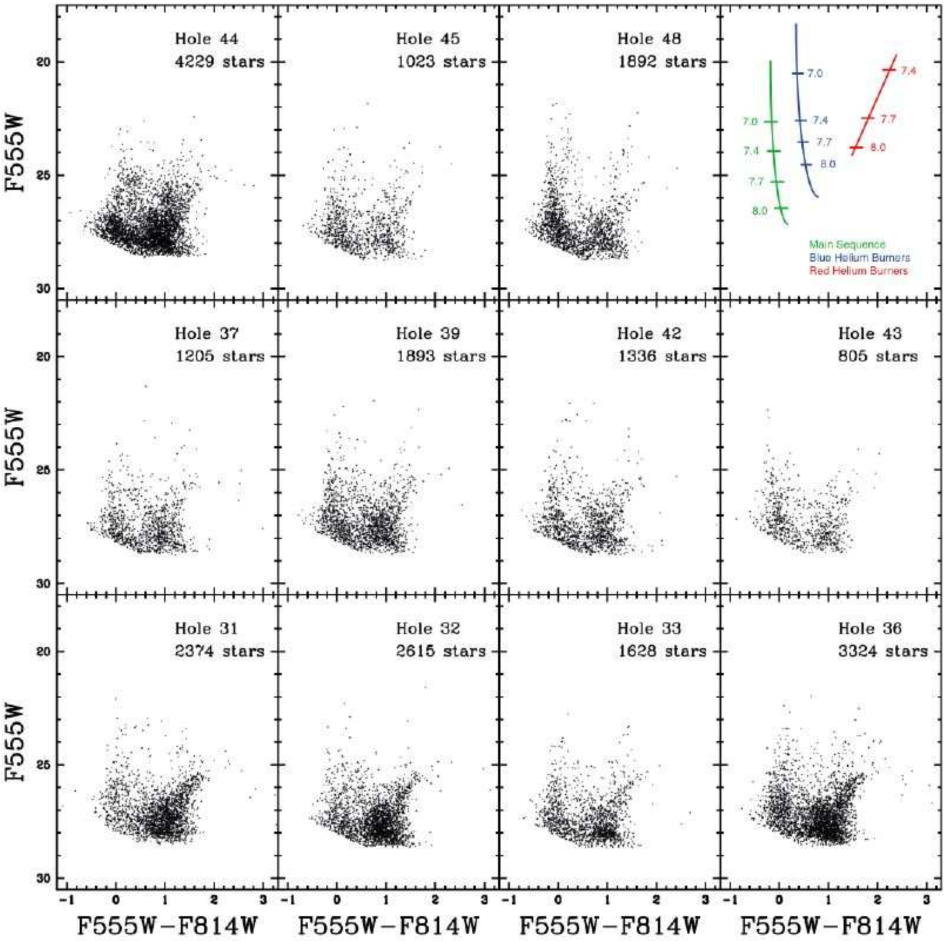

Fig. 25.— HST/ACS CMDs of the photometric apertures used by Rhode et al. (1999), corrected for foreground reddening, $A_V = 0.11$ (Schlegel et al. 1998). The schematic in the upper right hand corner shows the ages of each type of star, MS (green), BHeB (green), and RHeB (red), with the logarithm of the ages shown as a function of magnitude. Although sparse in some fields, note the presence of young MS and BHeB stars in all the CMDs. The fact the the BHeBs span a range in magnitudes indicate that multiple episodes of recent SF must have taken place, as different age BHeBs do not overlap on the CMD. In contrast, BHeBs from a single age cluster would have an overdensity at only one magnitude.

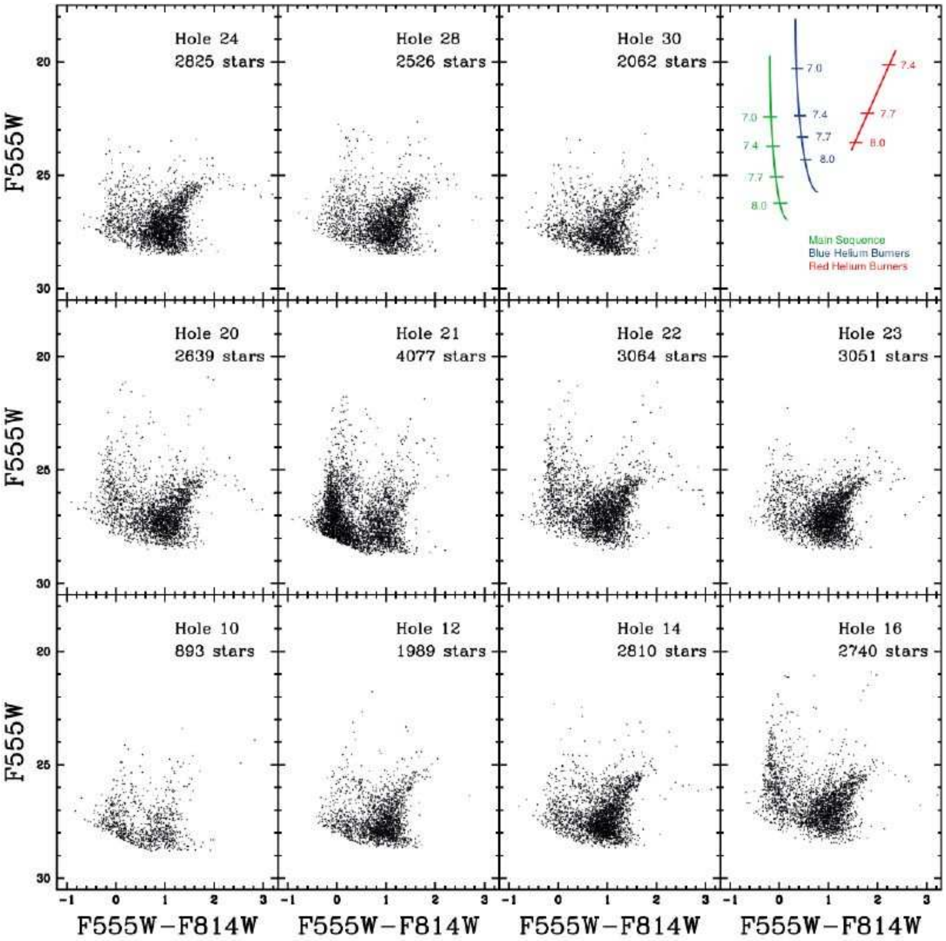

Fig. 26.— HST/ACS CMDs of the photometric apertures used by Rhode et al. (1999), corrected for foreground reddening, $A_V = 0.11$ (Schlegel et al. 1998). The schematic in the upper right hand corner shows the ages of each type of star, MS (green), BHeB (green), and RHeB (red), with the logarithm of the ages shown as a function of magnitude. Although sparse in some fields, note the presence of young MS and BHeB stars in all the CMDs. The fact the the BHeBs span a range in magnitudes indicate that multiple episodes of recent SF must have taken place, as different age BHeBs do not overlap on the CMD. In contrast, BHeBs from a single age cluster would have an overdensity at only one magnitude.

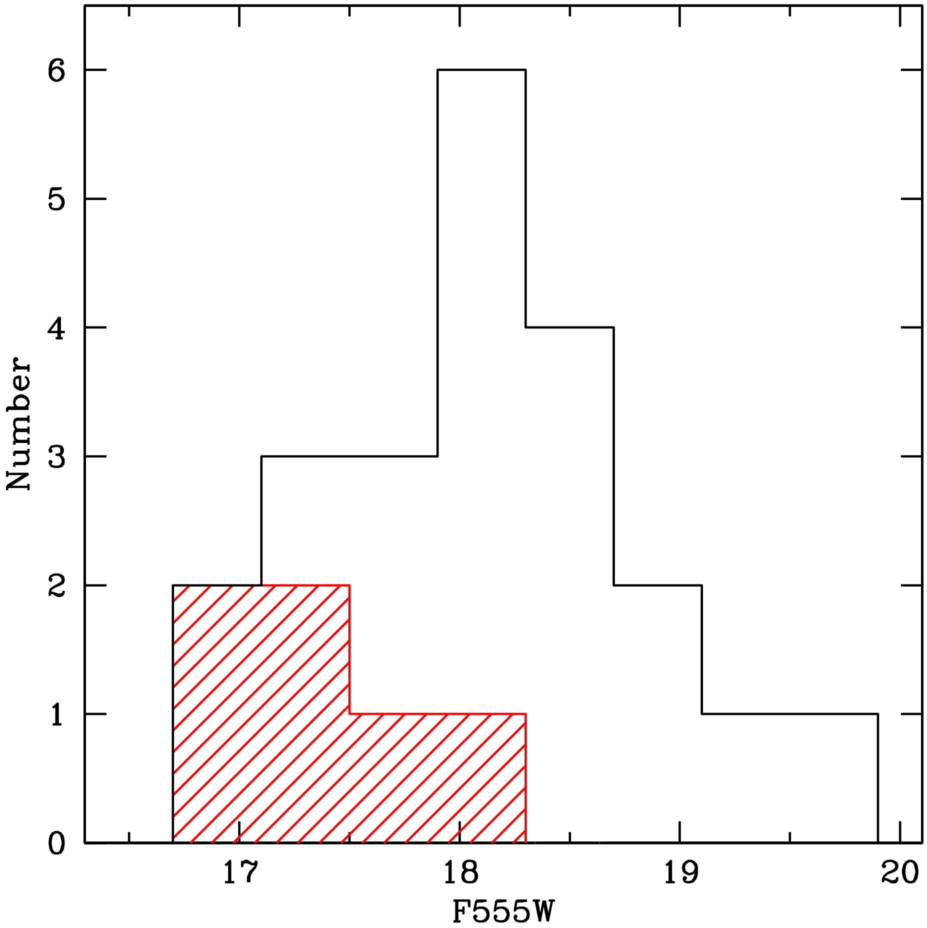

Fig. 27.— A histogram of the integrated ACS m_{F555W} magnitudes from the HST/ACS CMDs corresponding to the photometric apertures used by Rhode et al. (1999). The red shaded region represents the apertures that Rhode et al. (1999) classify as containing putative star clusters (Table 6). Note that they regions containing putative stellar clusters are among the brightest in the sample.

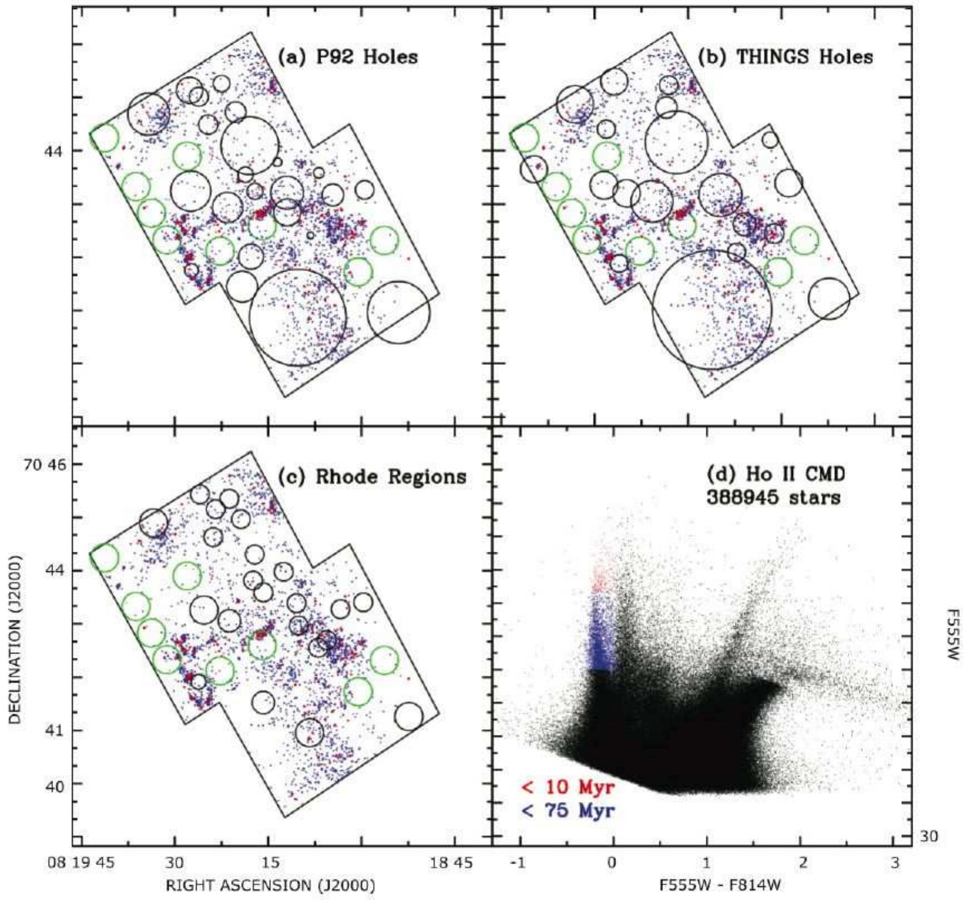

Fig. 28.— The spatial distribution of young MS stars (red < 10 Myr, blue < 75 Myr) plotted over (a) HI holes from the Puche et al. (1992) catalog; (b) HI holes from the THINGS catalog (Bagetakos et al. 2009); (c) photometric apertures of Rhode et al. (1999); Panel (d) is the CMD of the entire galaxy of Ho II with the young MS stars color-coded to match the spatial distributions with MS stars < 10 Myr in age in red and < 75 Myr in blue. Note the tendency of the red points to appear highly clustered, while the blue points are more widely distributed. Further, note that most of the HI holes do not contain highly clustered regions of young stars, rather these are found near the edges of the holes or near HI peaks.

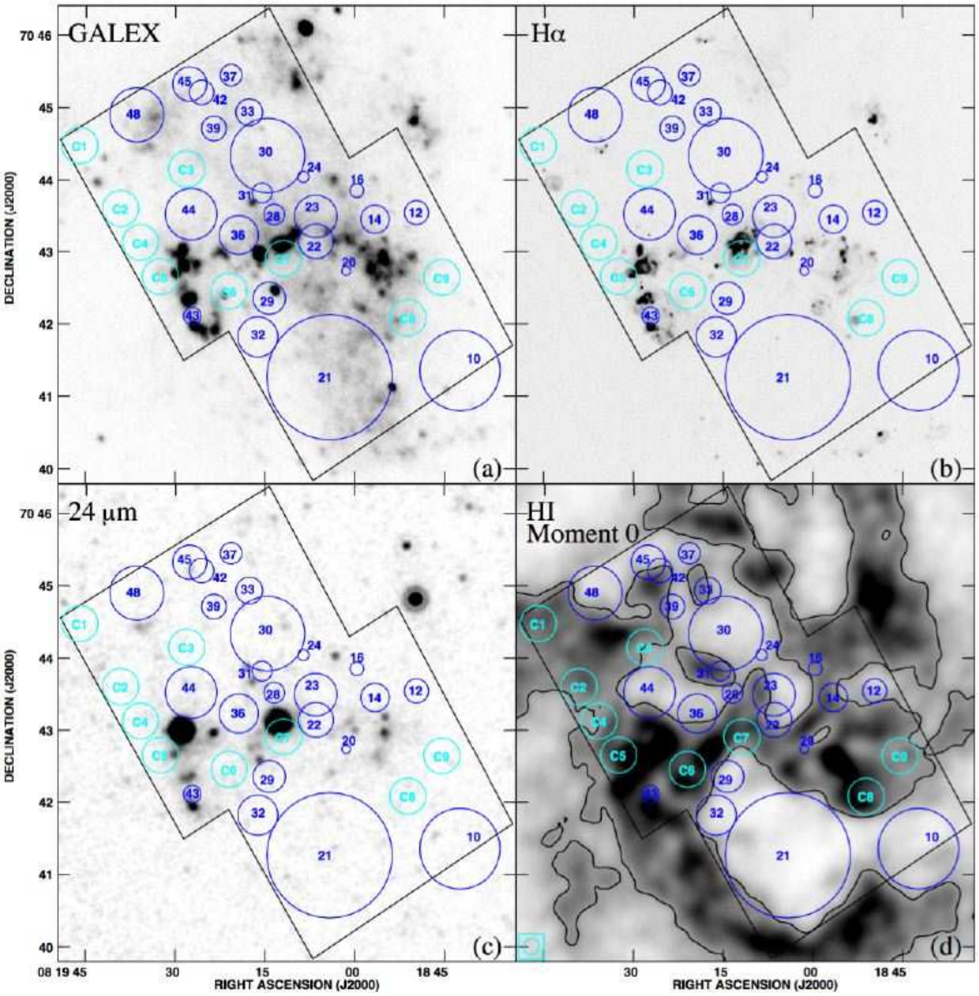

Fig. 29.— HI holes of Puche et al. (1992) (blue) and control fields (cyan) overlaid on Ho II images of (a) GALEX NUV (Gil de Paz et al. 2007); (b) LVL Hα (Lee et al. 2008); (c) SINGS 24μm Kennicutt et al. (2003); (d) THINGS HI (Walter et al. 2008). Despite that fact that all the HI holes contain hundreds or thousands of stars, from these images alone, it would seem that the HI holes are void of stars. At low SFRs ($< 10^{-4}$) $M_{\odot}$ yr^{-1}, it seems that these tracers of recent SF no longer reliably correlate with the underlying stellar populations (see §5.3 for further discussion).

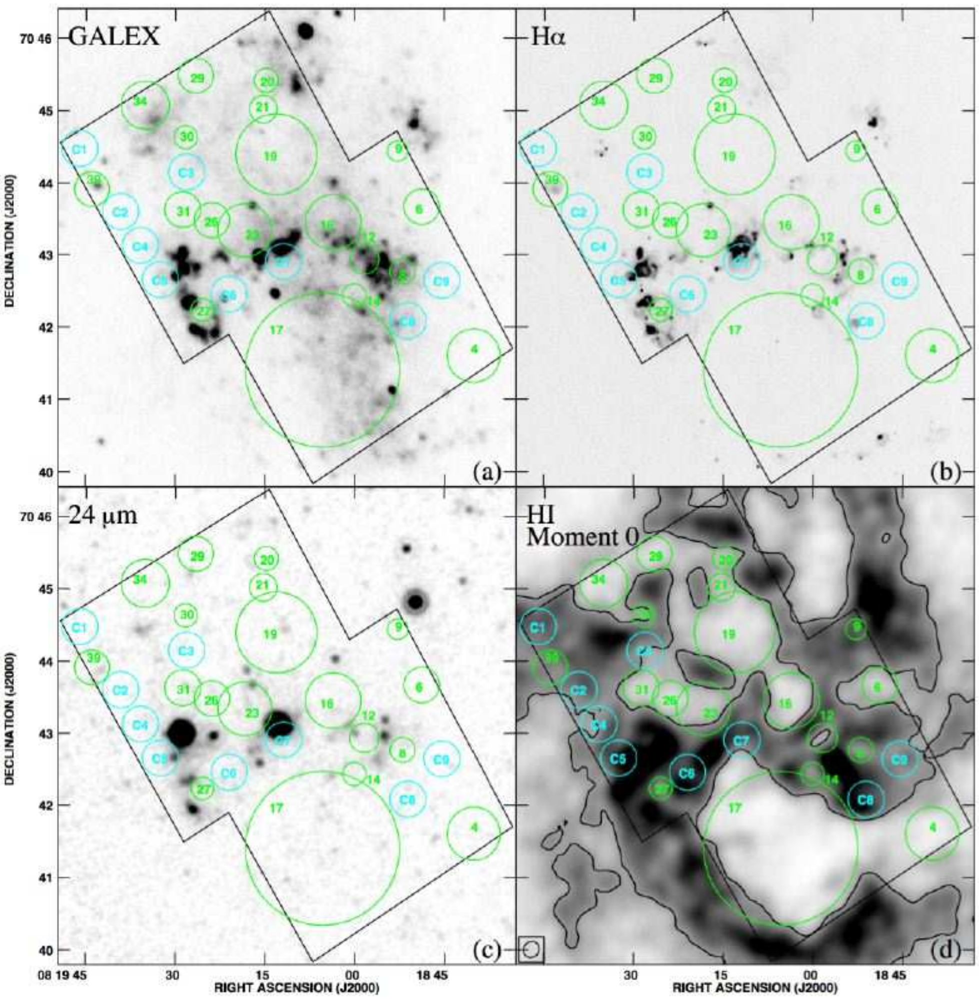

Fig. 30.— HI holes of Bagetakos et al. (2009) (green) and control fields (cyan) overlaid on Ho II images of (a) GALEX NUV (Gil de Paz et al. 2007); (b) LVL Hα (Lee et al. 2008); (c) SINGS 24μm Kennicutt et al. (2003); (d) THINGS HI (Walter et al. 2008). Despite that fact that all the HI holes contain hundreds or thousands of stars, from these images alone, it would seem that the HI holes are void of stars.At low SFRs ($< 10^{-4}$) $M_\odot$ yr^{-1}, it seems that these tracers of recent SF no longer reliably correlate with the underlying stellar populations (see §5.3 for further discussion).

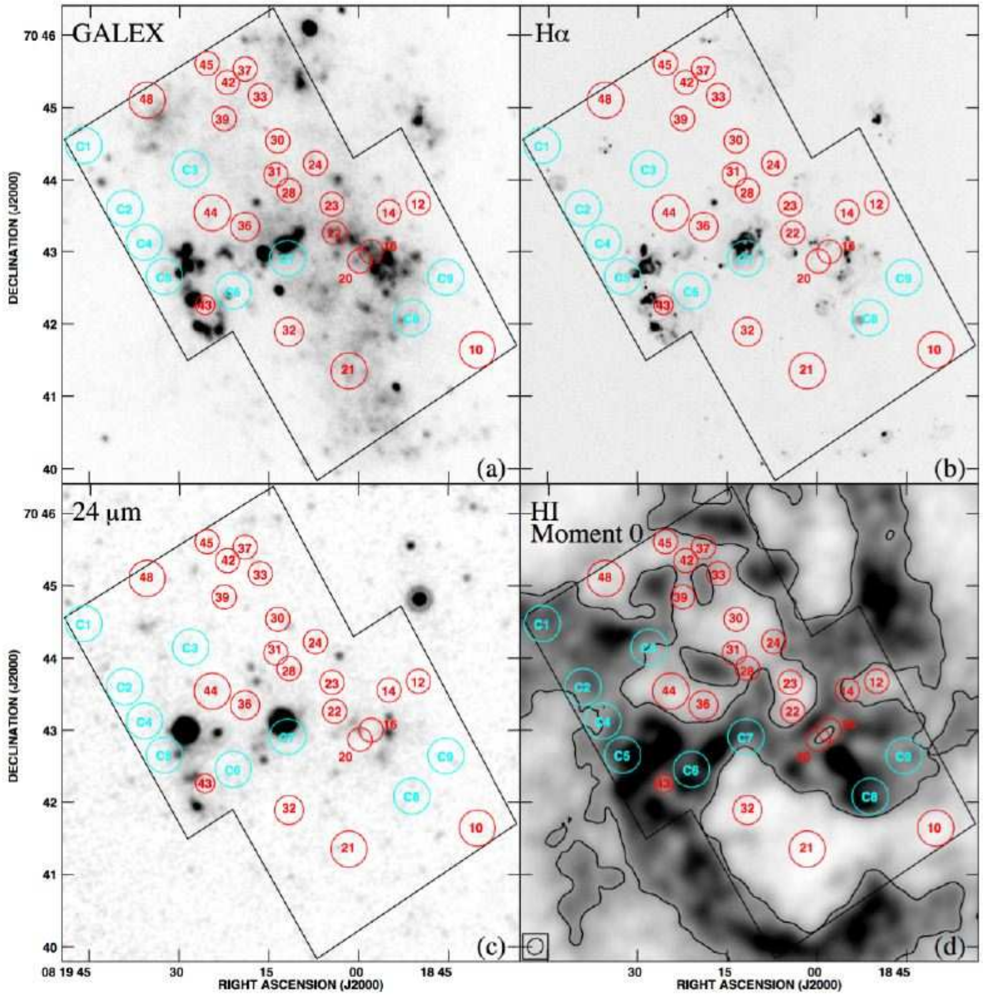

Fig. 31.— Photometric apertures of Rhode et al. (1999) (red) and control fields (cyan) overlaid on Ho II images of (a) GALEX NUV (Gil de Paz et al. 2007); (b) LVL Hα (Lee et al. 2008); (c) SINGS 24μm Kennicutt et al. (2003); (d) THINGS HI (Walter et al. 2008). Despite that fact that all the HI holes contain hundreds or thousands of stars, from these images alone, it would seem that the HI holes are void of stars. At low SFRs ($< 10^{-4}$) $M_{\odot}$ yr^{-1}, it seems that these tracers of recent SF no longer reliably correlate with the underlying stellar populations (see §5.3 for further discussion).

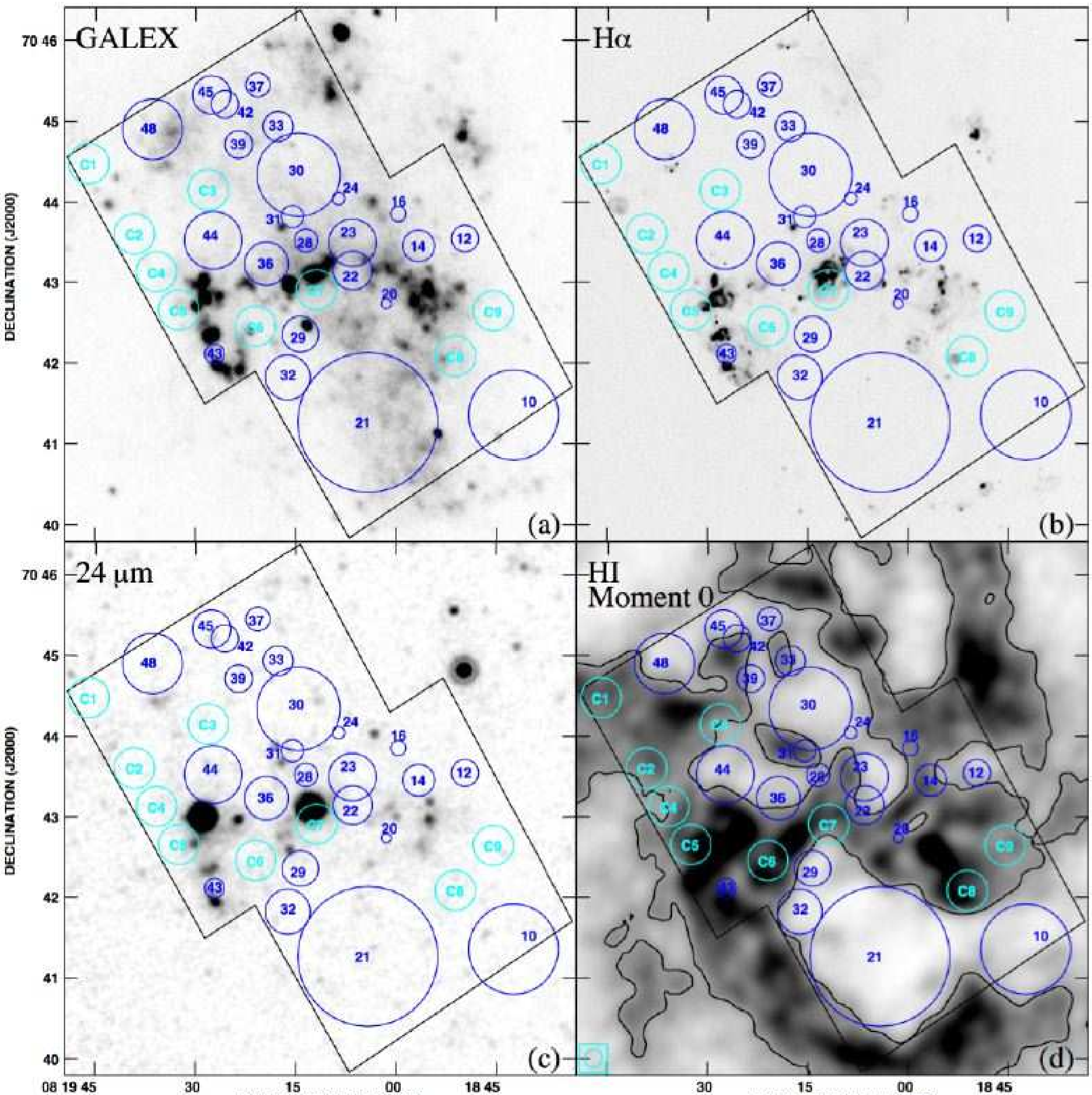
GALEX
Hα
24 μm
HI
Moment 0
(a)
(b)
(c)
(d)
DECLINATION (J2000)
RIGHT ASCENSION (J2000)
70 46
45
44
43
42
41
40
08 19 45
30
15
00
18 45
C1
C2
C3
C4
C5
C6
C7
C8
C9
10
12
14
16
20
21
22
23
24
28
29
30
31
32
33
36
37
39
42
43
44
45
48